N A S A C O N T R A C T O R
R E P O R T

NASA CR-137591

PIONEER JUPITER ORBITER PROBE MISSION - 1980

PROBE DESCRIPTION

by R.E. DeFrees

(NASA-CR-137591) PIONEER JUPITER ORBITER PROBE MISSION 1980, PROBE DESCRIPTION (McDonnell-Douglas Astronautics Co.) 51 p HC A04/MF A01 CSCL 22A

N78-33127

Unclas
G3/12 35922

Prepared by

MCDONNELL DOUGLAS ASTRONAUTICS COMPANY – EAST
St. Louis, Missouri 63166 (314) 232-0232

NATIONAL AERONAUTICS AND SPACE ADMINISTRATION • WASHINGTON, D.C. • 8 NOVEMBER 1974

FOREWORD

The results of a study to adapt the probe designed under Contract NAS2-7328, the Saturn Uranus Atmospheric Entry Probe (SUAEP) to a Jupiter entry probe is summarized in this report. The adaptation is tailored to a mission defined by the National Aeronautics and Space Administration - Ames Research Center and the European Space Research Organization. The material presented herein is to be integrated with a Pioneer derivative spacecraft and a propulsion module to facilitate a Pioneer Jupiter Probe Orbiter mission in 1980 ($PJ_P0'80$). This report is extracted from a comprehensive study of Jovian missions, atmospheric model definitions and probe subsystem alternatives to be published as NASA CR-137645, Feasibility Study of Low Angle Planetary Entry by R. E. DeFrees, McDonnell Douglas Astronautics Company-East.

TABLE OF CONTENTS

LIST OF PAGES

LIST OF FIGURES

INTRODUCTION TO THE JUPITER MISSION

A number of fundamental issues regarding the solar system can be clarified by means of atmospheric entry missions to the outer planets. Of these planets, Jupiter is the most attractive for atmospheric exploration. Jupiter has received the greatest attention from astronomers, so that new data can be fitted into the rich mosaic of previously obtained knowledge.

The specific information that we seek to know about Jupiter falls into four categories: planetary environment, energy sources, chemical composition and state of evolution. With regard to the planetary environment, ultra-violet radiation and energetic particles, which originate at the Sun, impinge on Jupiter's outermost atmosphere. The specific interaction between the planet and the incoming radiation is a function of Jupiter's particular chemical and electromagnetic properties. The incident solar radiation penetrates deep into the atmosphere before it interacts with the molecular constituents and is eventually converted into thermal energy. Due to its strong magnetic field, Jupiter is surrounded by an intense belt of highly energetic protons and electrons.

With the identification of hydrogen as the major chemical component of Jupiter's atmosphere has come a verification of the theory that this planet is very similar to the Sun in composition, but existing at much lower temperatures. Direct, accurate identification of the chemical compounds present in the atmosphere and measurement of their relative abundance and isotopic ratios can elucidate the chemical history of Jupiter from the time of its formation out of the primordial solar nebula.

Jupiter, Saturn and Neptune have the unusual characteristic of emitting much more thermal energy than they receive from the Sun. The data from the infrared radiometry experiment on Pioneer 10 indicate that Jupiter emits over twice the incident solar radiation. The identification of the sources of this emission and the radiative mechanism by which it is generated may prove that Jupiter is a stillborn star or one in the last stages of decay.

A strong case for Jupiter atmospheric entry missions can be made in terms of the questions that will remain unresolved even after the Pioneer 10 & 11 flyby missions. On the basis of the Principal Investigators' analyses of Pioneer 10 Jupiter data, it appears that the infrared photometry and radio occultation experiments are unable to provide a precise description of Jupiter's atmosphere. The obstacles to defining Jupiter's atmosphere by means of remote

flyby experiments arise from the dense opaque nature of the atmosphere. In the case of optical spectroscopy, the spectra of the atmosphere has proved to be very difficult to interpret, especially in the infrared. There are an enormous number of weak lines in the spectra for which we cannot ascertain corresponding quantum states. The presence of aerosols in the atmosphere compounds the difficulty of interpreting the spectrum. These particles tend to scatter the incoming solar light, causing the path of an incident photon to be quite complex. Also, the scattering power of the aerosols exhibit a wavelength dependence. Therefore abundance estimates require measurements of lines of comparable intensity in the same region of the spectrum and result in relative rather than absolute abundances.

Radio occultation is also of limited usefulness. In very dense atmospheres, such as Jupiter's, extinction of the radio signal is caused by excessive defocusing attenuation within the atmosphere. In the case of Jupiter extinction, this occurs at a pressure level for S-band of 2.8 bar. Below this level no further tangential penetration by radio rays is possible. Because our ground-based and flyby measurements are susceptible to various conflicting interpretations, in situ measurements of local physical properties and chemical composition within the atmosphere are needed to remove the dependence on atmospheric modeling and lead directly to the utilization of prior remotely acquired data.

The types of experiments that have the highest priority for in situ measurements on an entry probe are concerned with atmospheric structure and chemical composition. A tri-axial accelerometer provides data on atmospheric densities. These data, when combined with direct low altitude measurements of ambient temperatures and pressures, provide profiles of the physical structure of the atmosphere. The chemical composition of the atmosphere is determined by mass spectrometry and gas chromatography. These data are gathered in the troposphere, where the atmosphere is homogeneous.

The atmosphere of Jupiter can be successfully explored in the early 1980's because of three major developments. These developments have come to fruition through the combined efforts of the National Aeronautics and Space Agency, the aerospace industry, and individual researchers. By utilizing the technology gained while carefully proving each element of the configuration step by step,

an atmospheric probe can be available for launching in 1980 on an interplanetary spacecraft.

The three developments that have produced this feeling of confidence are:

1) The characterization of the Jovian magnetosphere by Pioneer 10 which permits more accurate prediction of component environments. Knowing the nature and severity of the exposure, functional elements can be hardened to survive the effects of trapped particle radiation. The exact character of the environment is still incomplete within the 3 to 1 R_J layer, but the planned passage of Pioneer 11 will improve current modeling in this layer, thereby permitting thorough analysis of protection needed and already provided.

2) The refinement in ephemeris resulting from the Jupiter flyby in 1973 by Pioneer 10. The precision in knowing Jupiter's mass properties and its locus as a function of time permits accurate planning of an atmospheric entry mission at a few degrees flight path angle from the skip-out boundary. By keeping the angle low, the heating environment can be accommodated with current state of the art thermal protection materials. Although entry conditions into the Jovian atmosphere are the most severe of any planet, the combination of precision in trajectory targeting and material fabrication assure survival through the peak heating environment.

3) The evolution of convolutional coding techniques and communication linkages that can operate in a noisy, turbulent environment at or above the adverse tolerances present at the outer planets. Again, each planet's synchrotron noise and other conditions which influence communicability are not completely understood. The level of understanding and the tools to overcome the problems have evolved to the point where alternative solutions can be defined and selection criteria established. These in turn will permit the development of a workable link when needed.

These anticipated hazards (trapped particles and entry heating) are considered to be tractable at this time. The remainder of this report is directed at detail examination of the design problems foreseen and solutions which, as yet, are not necessarily optimal. Continuing study will reveal alternative paths over or around the hazards. The work described has been performed by the McDonnell Douglas Astronautics Company-East under contract to Ames Research Center. An extensive report of the studies is to be released about 1 January 1975 and discusses many aspects of Jovian entry strategies.

MISSION ANALYSIS

The spacecraft and probe are targeted at the probe entry point as depicted in Figure 1. At a distance from Jupiter that is within its sphere of influence, herein taken at 500 R_J, the probe is released. The spacecraft is retargeted via a deflection maneuver for a near overfly of the probe by the spacecraft, this is phased to occur during the probe's data gathering descent into the Jovian atmosphere and prior to spacecraft insertion into orbit. Phasing is accomplished during the deflection and consists of a deceleration of the spacecraft to cause a lag. The probe mission is completed when the probe and spacecraft are no longer in communications view of each other.

OPP-3

MISSION CHARACTERISTICS

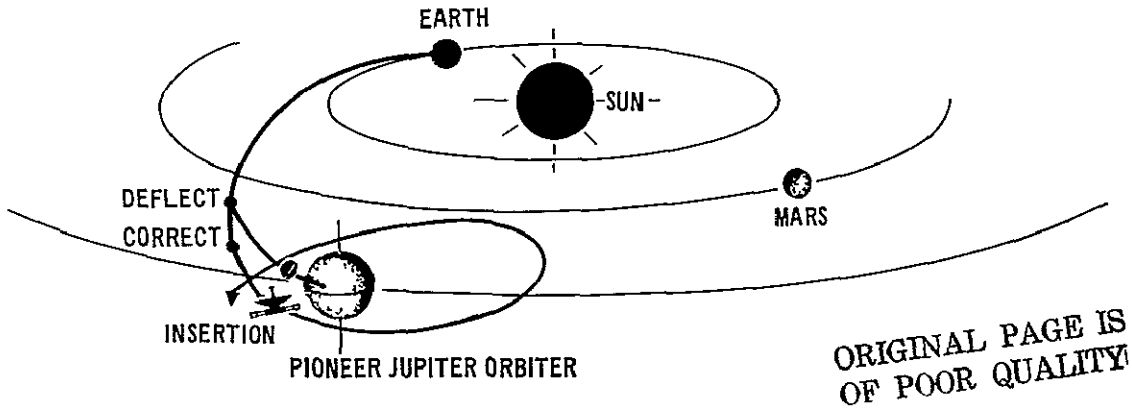

LAUNCH DATE	6 DEC 80	PROBE ENTRY	
ARRIVAL DATE	14 FEB 83	ALTITUDE	450 km
SEPARATION MANEUVER	500 R_J	PATH ANGLE	−7 5 deg
DEFLECTION ΔV	71.05 m/s	LATITUDE	4.71 deg (N)
TIME TO PROBE ENTRY	50 DAYS	VELOCITY	59 7646 km/s
CORRECTION MANEUVER	260 R_J	ANGLE OF ATTACK	16 63 deg
CORRECTION ΔV	5 m/s		
TIME TO PROBE ENTRY	23 4 DAYS		

Figure 1

In the cruise mode the Pioneer spacecraft is spin-stabilized along the Earth-line direction to retain communications lock with the Earth. During the probe separation and spacecraft deflection maneuvers, retention of Earth communication lock (spin-axis alignment along the Earth-line) can be retained or the spacecraft/probe can be precessed for optimum release attitude and/or optimum deflection maneuver direction application. Probe attitude and, thereby,

entry angle of attack are established by the spacecraft orientation at separation. When Earth communications lock is retained, the spacecraft deflection maneuver must be implemented as two separate maneuvers; one applied along the spacecraft spin-axis and the other a pulsed maneuver applied normal to the spacecraft spin-axis. When Earth communications lock is broken (second option), a single deflection maneuver applied along the precessed spin-axis in the optimum direction is utilized. Both techniques provide acceptable entry conditions for the probe.

At a nominal separation/deflection radius of 500 R_J, the spacecraft Jovian latitude can be held to +0.02 degrees (North). Thus, probe injection into a near-zero inclination trajectory (and eventually spacecraft insertion into a near-zero inclination orbit) is achievable as part of the deflection maneuver implementation as seen from the equatorial plane depicted in Figure 2.

PROBE AND SPACECRAFT APPROACH TRAJECTORIES

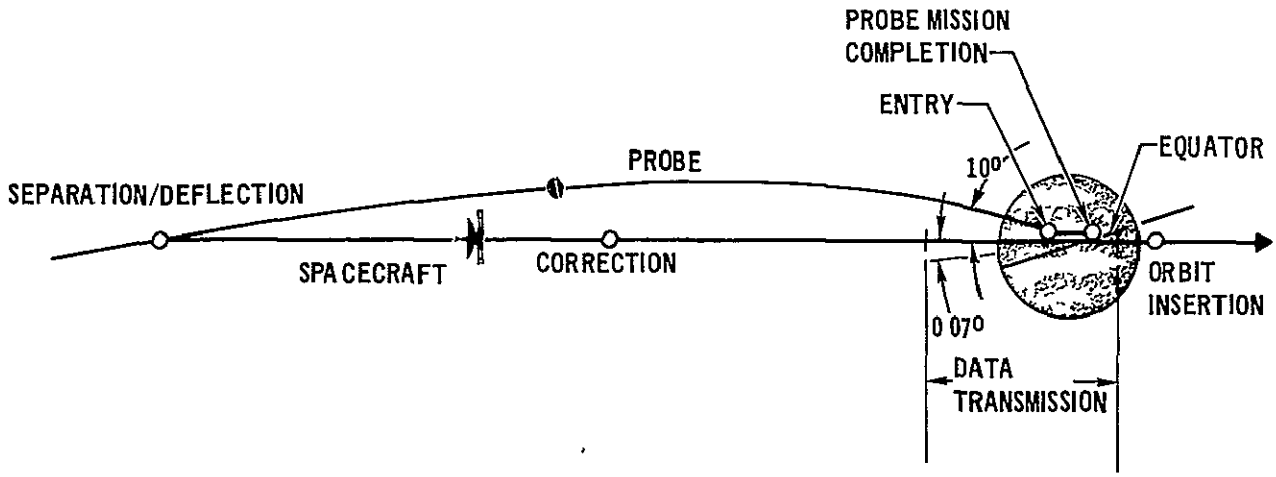

Figure 2

The environment of Jupiter is considered to be hazardous to an entry probe in two principal ways: (1) The particles that are trapped in the magnetosphere, and (2) the entry heating encountered in the atmosphere. The radiation emitted by the trapped electrons and protons can be minimized by synchronizing the

approach to penetrate the wobbling magnetodisc at a favorable time. A typical trajectory for the probe was established to permit analysis of the radiation dose to be encountered by a probe. The dose rates as a function of radial distance for the trajectory are plotted in Figure 3. By parametrically choosing different phasing angles for passage through the particle belt, a total dose can be obtained. The results of this analysis are illustrated in Figure 4. They show a distorted sine wave and a variation of up to four in total dose. Each curve represents the exposure dose that an entry probe would experience during a descent; the differences between curves demonstrates the effect of phasing the entry path with the wobble of the magnetodisc. It is apparent from the absolute values shown that synchronizing the approach to alleviate this exposure is a mission constraint that should be imposed. Fortunately, the planet rotates rapidly, so imposition of a specific phasing does not overly restrict the available entry windows.

OPP-37

JUPITER DOSE RATE PROFILES FOR DIFFERENT PHASING ANGLES

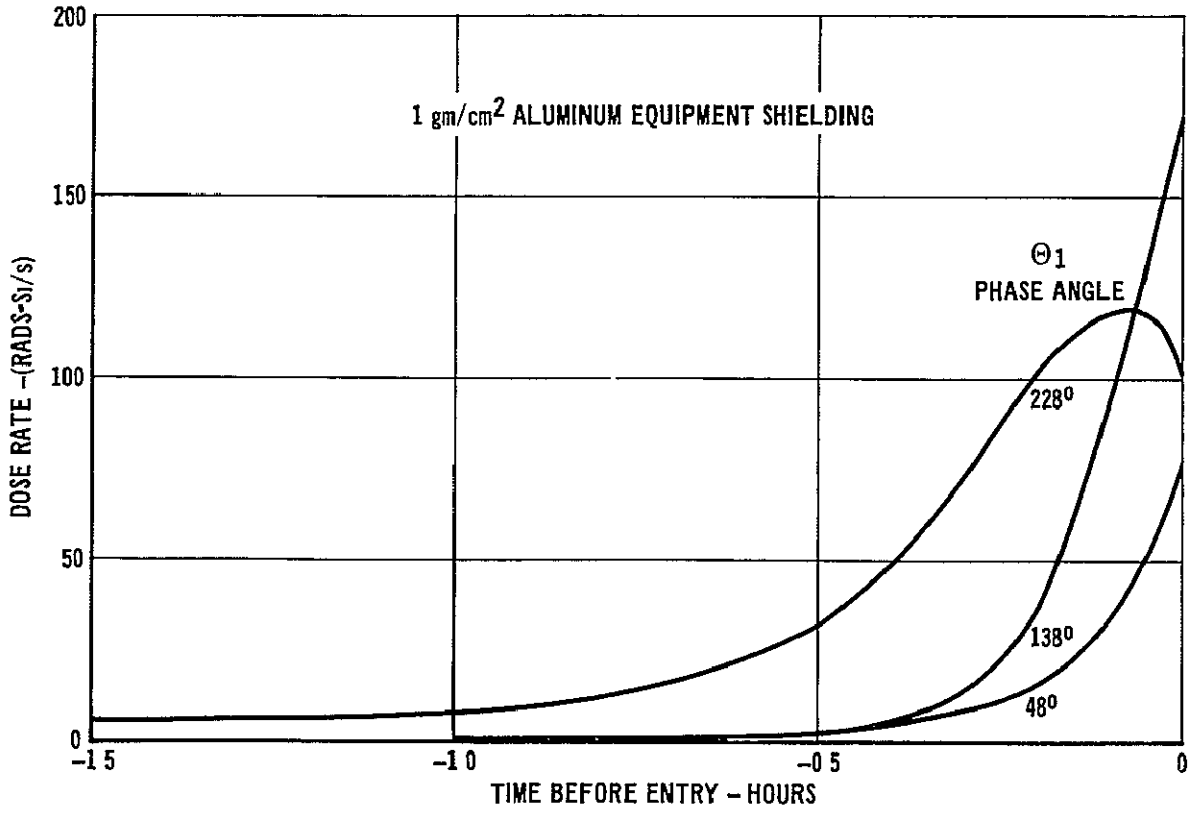

Figure 3

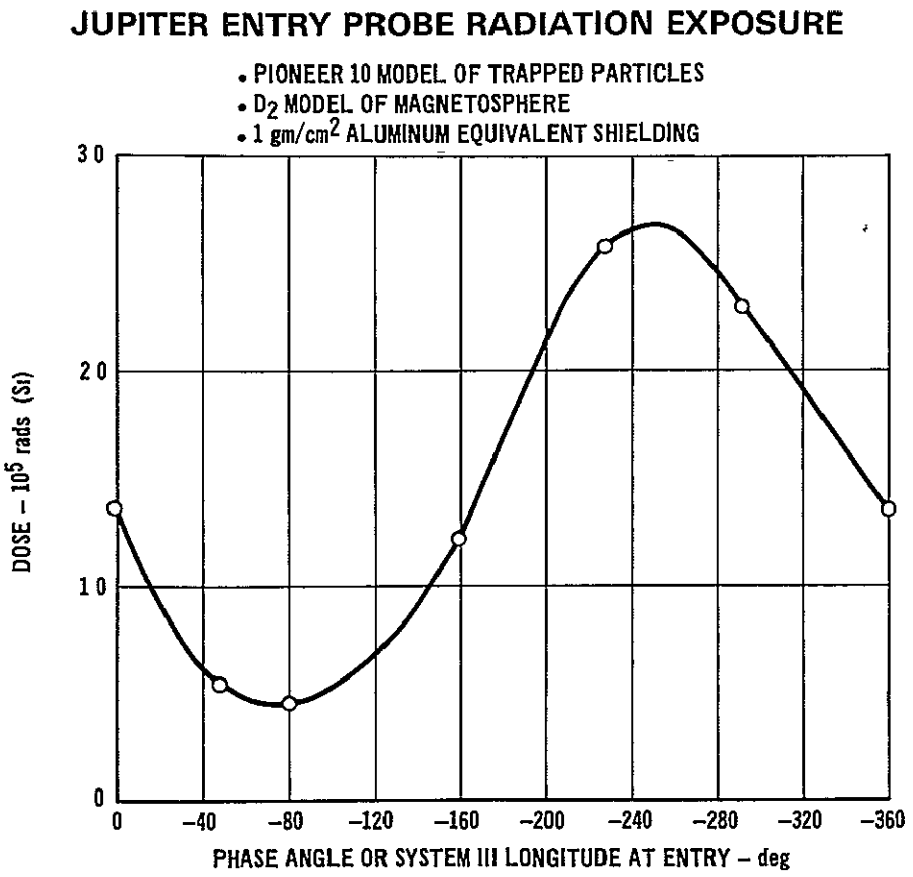

Figure 4

The structure of the probe inherently contains some shielding for the electronics. The packages by and large are all within a thick carbonaceous and metallic cone that extends well back. The most vulnerable direction is aft where the materials provide very little mass shielding. The more energetic particle radiation will pass through to the equipment section. A rigorous study is underway on the shielding provided by metal boxes and other materials, jointly by TRW and McDonnell Douglas Astronautics. The study will proceed to selection of internal components that are resistant to high energy radiation.

Following separation from the Pioneer spacecraft, the probe passively descends to a shallow angle entry into the Jovian atmosphere while the spacecraft is deflected for a near overfly of the probe and insertion into a low periapsis (taken at 1.8 R_J), low inclination (0.07 degree) Jovian orbit (see Figure 2).

Since errors accrued during the spacecraft deflection maneuver result in intolerably large dispersions in communications geometry, a spacecraft correc-

tion maneuver is incorporated into the spacecraft descent trajectory profile to bring these dispersions within manageable bounds (by a factor of 1/9th). If this correction maneuver is performed near the mid-descent point, which nominally takes place at 260 R_J, adequate time is available for tracking the spacecraft's path. The post-deflection maneuver trajectory is determined and the ΔV requirements computed to retarget spacecraft periapsis radius. The ΔV size of this maneuver is of the order of 5 m/sec which is a part of the normal deflection maneuver ΔV budget.

The probe is nominally targeted to a 4.71 degree (equatorial north) latitude, posigrade entry point with an inertial entry path angle of -7.5 degrees. Note that the probe entry altitude callouts are referenced to the equatorial radius of 71422 km. Since the probe attitude is established by spacecraft attitude at separation, retention (or nonretention) of Earth communications lock directly determines probe attitude and, thereby, the angle of attack at entry. When the Earth-lock communication option (spin-axis aligned along the Earth line) is retained, the relative angle of attack at entry is 16.63 degrees. Naturally, when communication-lock is broken (second option), a zero degree entry angle of attack can be achieved.

The mission profile assumed for this study is summarized in Figure 5. The probe data transmission period and the spacecraft orbit insertion burn can be kept separate at a small cost in non-optimal insertion burn propellant.

Communications geometry between the spacecraft and probe is represented by spacecraft and probe aspect angles, communications range and communications duration. As depicted in Figure 6, spacecraft aspect angle is taken as the angle, measured at the spacecraft, between the probe line-of-sight and the spacecraft spin axis (i.e., along the Earth-line but away from the Earth direction in the cruise mode). Probe aspect angle is the angle between the spacecraft line-of-sight and the probe spin axis measured at the probe. Prior to atmospheric tip-over the probe spin axis is along the Earth-line when the Earth lock retention option is used, thus, until tip-over both aspect angles are virtually the same. Communications range is the distance between the probe and spacecraft. Communications duration is taken as the time from probe entry until communications geometrical constraints are violated; about 25 minutes is currently predicted. The duration can be varied by firing along the spacecraft trajectory path to retard it, but any gain is obtained at great expense.

MISSION PROFILE FOR JUPITER PROBE

OPP-2

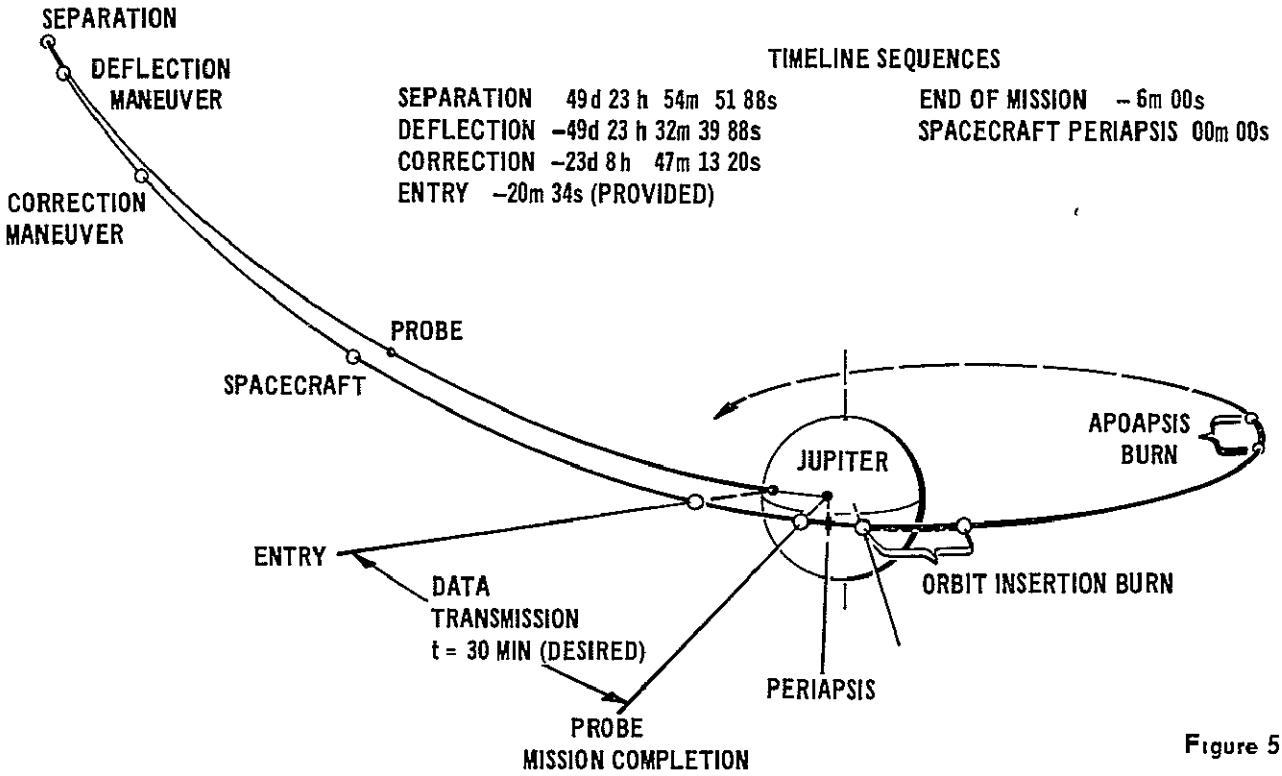

Figure 5

COMMUNICATIONS GEOMETRY

OPP-18

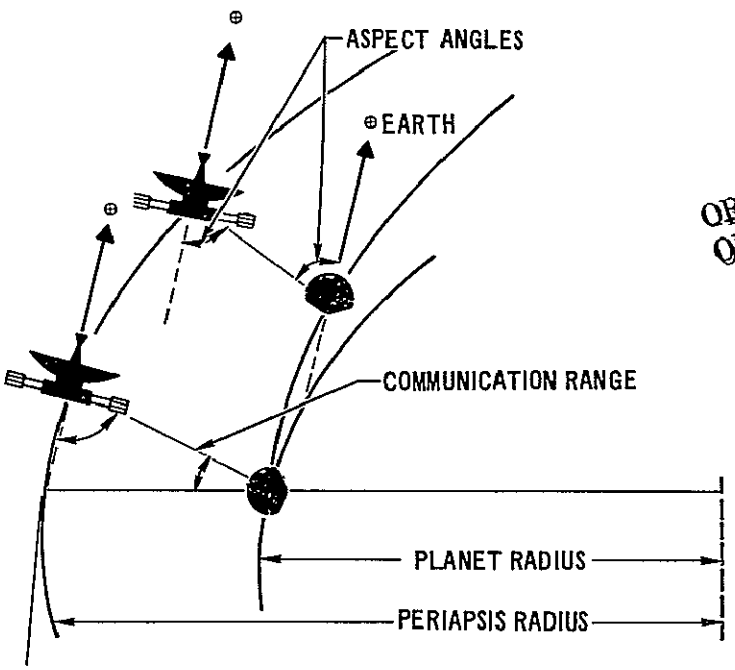

Figure 6

Two other parameters commonly used for these communications geometry studies are spacecraft periapsis radius and spacecraft phasing time. Periapsis radius refers to the trajectory periapsis of the spacecraft after the deflection and correction maneuver which in this instance occurs prior to orbit insertion. Phasing time is the time past entry when the spacecraft is phased to pass closest to probe zenith. Even if both vehicles retain the same inclination, the spacecraft will not necessarily pass directly overhead because the probe moves latitudinally after entry into the planet's atmosphere.

The probe enters the atmosphere at a total angle of attack which is dependent upon the spacecraft/probe separation conditions. Upon entry into the planet's sensible atmosphere, the descent trajectory and aerodynamic properties will determine the probe's motion characteristics. Clearly, the motion-time history during hypersonic descent must be well established for the mission to ensure small angles of attack during peak heating and subsonic motion characteristics which are consistent with communications and science constraints. A six-degree-of-freedom trajectory analysis (which incorporates aerodynamic force-moment and stability test data) was used to predict the motion-time history for the Jupiter mission. Figure 7 presents the results obtained for two different

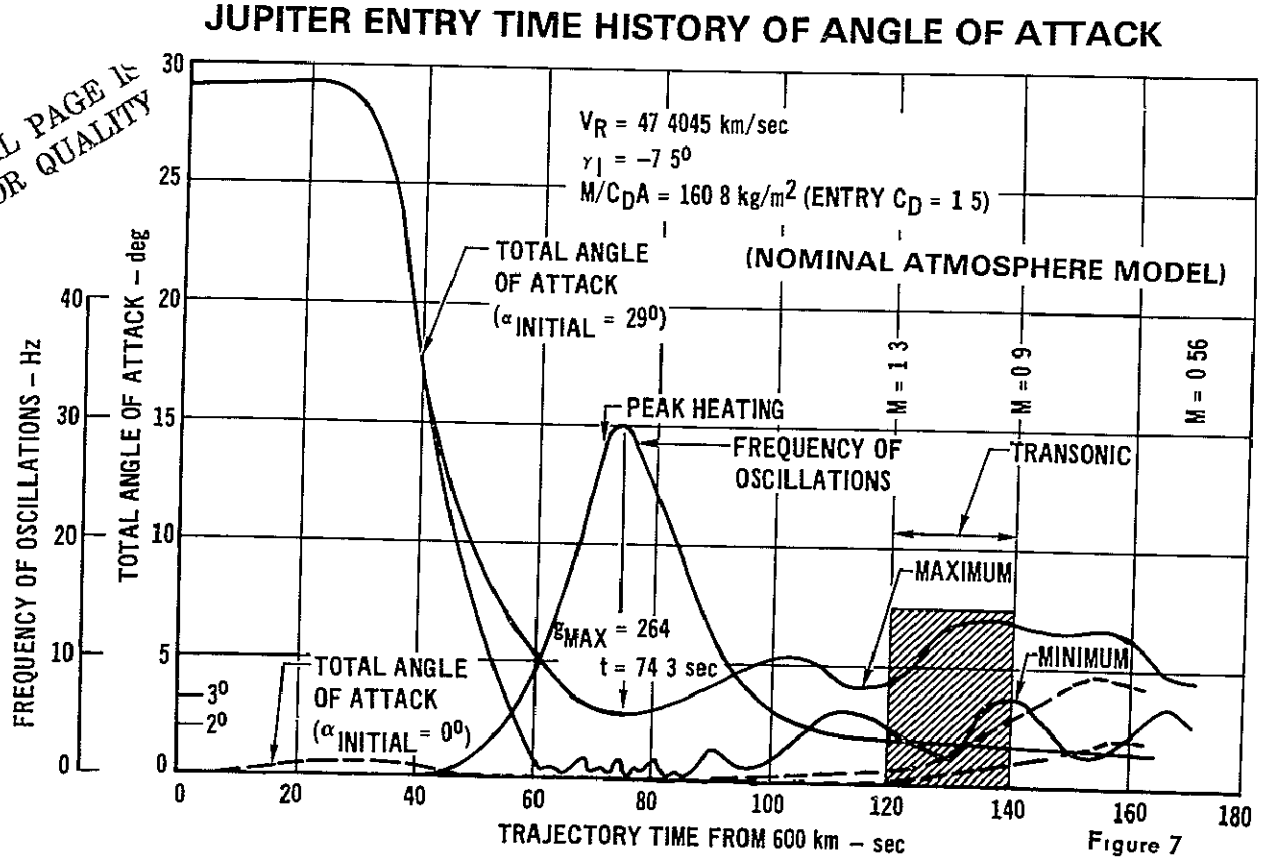

Figure 7

initial angles of attack; the 29° entry is associated with a Pioneer mission which maintains Earth-lock during probe separation while the 0° case reflects the entry angle of attack if the spacecraft breaks Earth-lock. Both calculations indicate low subsonic limit cycle oscillations (less than 7°) which are satisfactory for providing a solid platform for science measurements and which do not significantly degrade the communications subsystem. Entry at zero degree angle of attack results in a near zero degree angle at peak heating while the Earth-lock case exhibits a maximum angle of attack of 2.75 degrees at peak heating. The higher angle of attack at peak heating results in asymmetrical ablation and a lateral shift in the probe's center of gravity. Neither the severity nor the effects of the nonsymmetrical ablation have been assessed, as yet, but subscale tests of ablation are underway at Ames Research Center and at the McDonnell Douglas Astronautics Company.

The descent time history of a point mass is extended in Figure 8 to the terminal conditions. The entry flight path angle of -7.5 degrees limits entry

DESCENT TIME HISTORY
JUPITER NOMINAL ATMOSPHERE

OPP-16

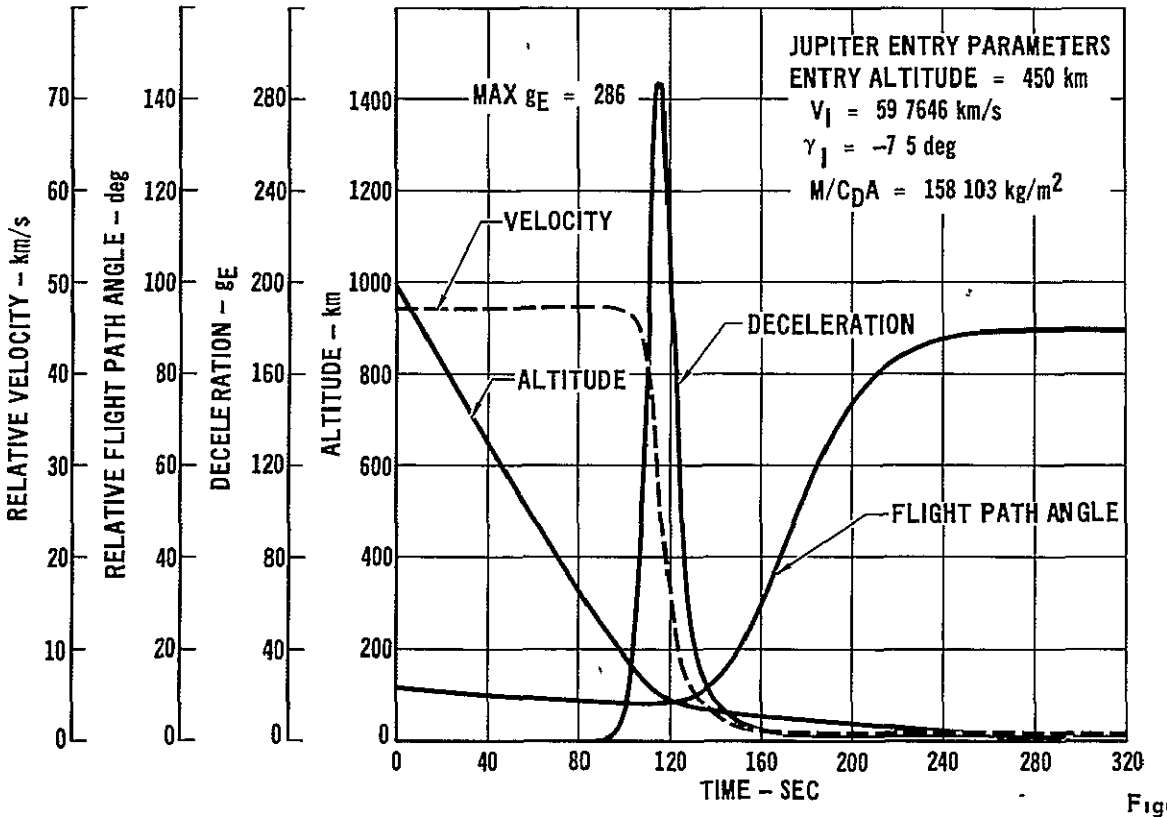

Figure 8

decelerations to the 300 g_E level which is well within the design value. The tip-over condition is completed by 5 minutes after entry.

The conclusion is drawn from this analysis that the entry probe design can be adapted to be compatible with a Pioneer spacecraft orbital mission to Jupiter in 1980 with only peripheral changes. Additional study is required to optimize the trajectory to limit radiation effects and entry heating while fulfilling scientific data gathering and handling functions.

PROBE DESCRIPTION

The Jupiter probe design emphasizes use of current technology and flight proven materials, hardware, subsystems, and components. The design stresses development through exploitation of existing testing and research facilities, established fabrication processes and proven aerospace methods. The probe's size, shape and internal arrangement is not optimized for minimum weight; but instead, for maximum development confidence. The goal is to achieve low technical risk through conservatism and moderate overdesign to increase development confidence with minimum cost and through simplifications which preclude sophisticated validation testing.

Most of the structure, mechanisms, internal support, and other components (see Figure 9) have already been fabricated in ARC machine shops. A full-size engineering model, complete with installed ballast equipments, simulated heat loads, wire bundles, and insulation will be completed and available for structural, vibration, and thermal test validation early in 1975. A quarter size carbon-phenolic forward heat shield has been fabricated, and a full-size heat shield is scheduled for fabrication next year. This heat shield will be used on the engineering model. Many design validations, including sample inlet and contamination tests,mechanical systems tests,heat shield specimen characterizations, insulation characterizations, structural tests, vibration and shock tests, thermal tests, aerodynamic stability validations, antenna patterns, and communication simulations are also underway.

The major features of the Jupiter entry probe are illustrated in Figures 9 and 10. The probe is a compact, blunted 60° half-angle cone forebody and a hemispherical afterbody. The forebody is a single piece, machined carbon-phenolic sphere-cone 889 mm (35 in) in diameter. The afterbody is a fiberglass-phenolic honeycomb hemisphere (45 cm spherical radius) filled with a low density elastomeric ablation material. The forward ablator is a 5.35 cm (2.1 in.) thick carbon phenolic of 1441 kg/m^3 (90 lb/ft^3) density. The billet for this heatshield is made by layering carbon-phenolic cloth and forming it under heat and pressure up to 690 N/mm^2 (1000 psi). The heat shield is sized to dissipate the Jupiter entry heat load (primarily by ablation) that is calculated for a Jupiter Nominal atmosphere at an entry angle of -7.5 degrees.

PROBE CONFIGURATION

OPP-13

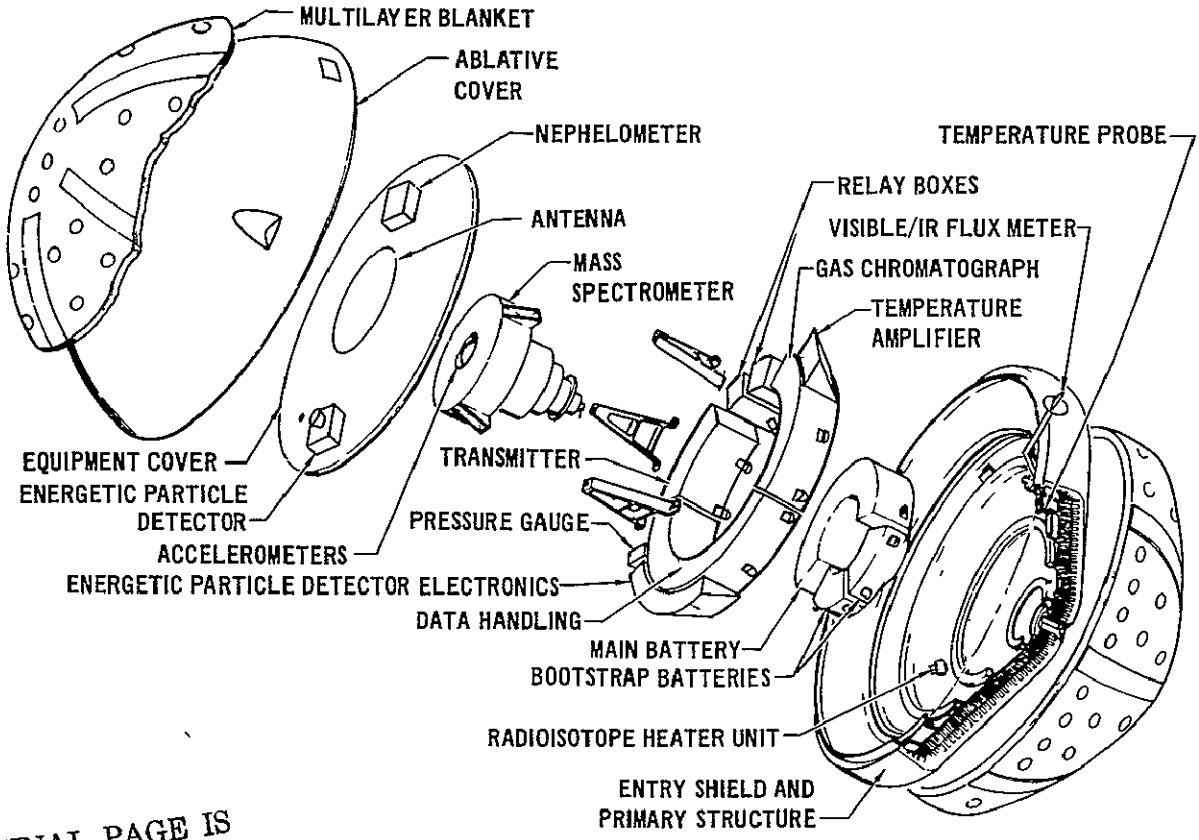

Figure 9

Two ejectable plugs are fitted into the heat shield. One is located at the center of the sphere-cone and accommodates the extension of the atmospheric sampling tube for the mass spectrometer, the gas chromatograph and the total pressure gage. The other plug allows the extension of the atmospheric total temperature sensor and is located on the conical section. Initiated by the appropriate accelerometer input,both plugs are ejected after maximum entry heating and at subsonic free-fall velocity.

The probe's primary structure is a 1.52 mm (.060 in.) aluminum (7075-T351) cone (coolie hat) with 5 integrally machined concentric rings. This structural cone is machined from a formed conical billet 5.1 cm (2 in.) thick. The two outermost rings are closed to form a box ring section by mechanically attaching a pressed "L" ring of 7075-T351 aluminum sheet stock (.063 in.). This outer

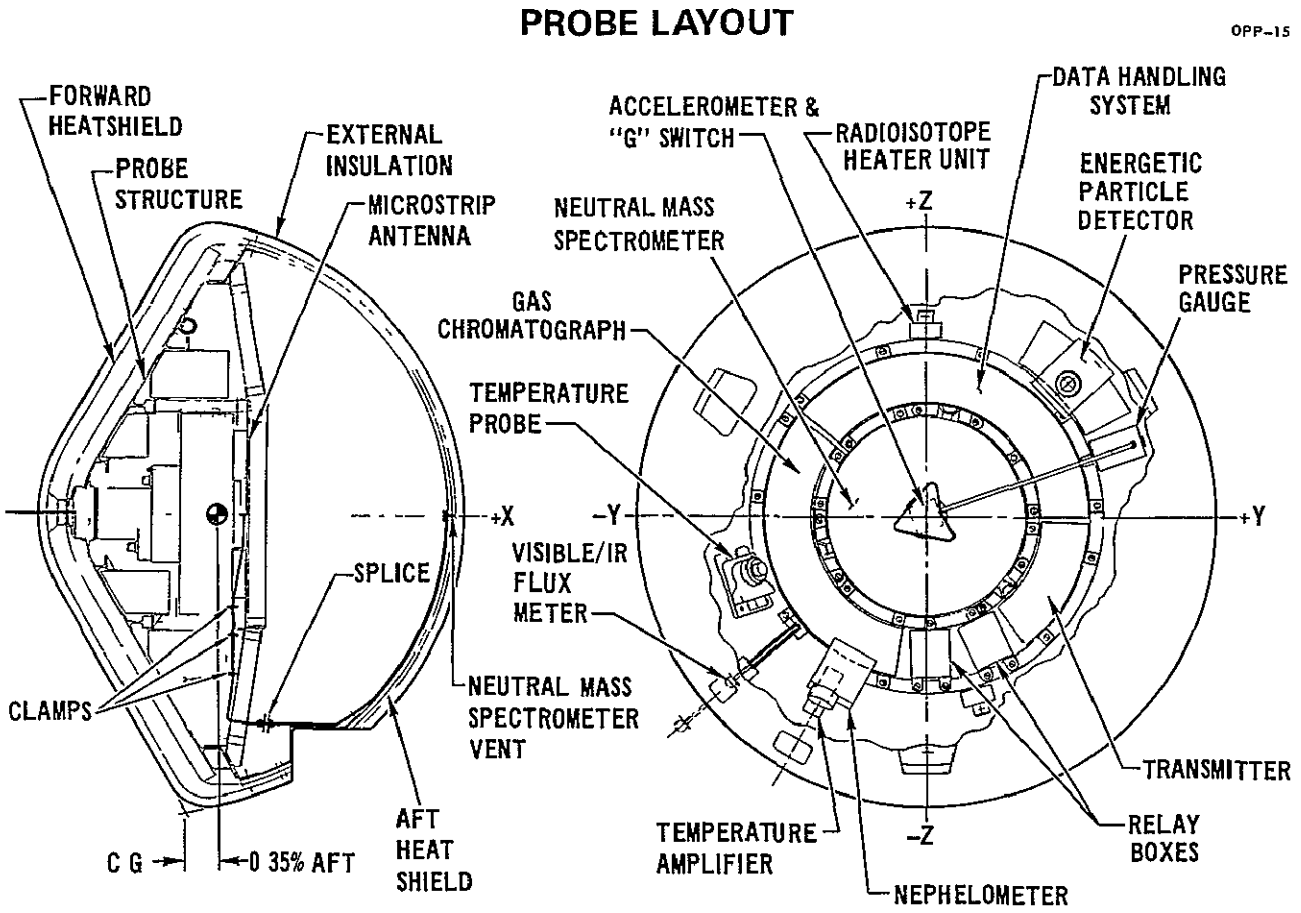

Figure 10

box ring is the major structure to which the afterbody is attached (31 circumferential bolts). All fasteners used in the probe are titanium. Attachment to the Pioneer spacecraft is at 3 stainless steel attach fittings located 120° apart around the afterbody. The recessed attach fittings are bolted to the fiberglass honeycomb afterbody dome. Launch loads are transmitted through the 3 attach fittings, and the loads are distributed to the primary structure at the outermost box ring. The three inner machined rings support the bulk of all the probe's support equipment and the instruments. A 2.15 cm (.85 in.) thick 1/4 8.5 fiberglass honeycomb core is bonded by a high temperature adhesive to the outer surface of the machined aluminum cone. The fiberglass-phenolic honeycomb core has an outer fiberglass facesheet 1.27 mm (.050 in.) thick. The machined one piece carbon-phenolic heat shield is bonded to this face.

The primary structure described above is designed for entry decelerations of 800 g_E with a safety factor of 1.25. The bonded attachment of the heat shield to this structure is not considered additive to the structural strength. The nearly circumferential arrangement of the component containers distributes the individual inertia loads to the conical honeycomb structure almost uniformly. These individual loads are uniformly balanced by the atmospheric pressure loads that impinge on the heat shield face during entry, so that a minimum of bending is present on either the carbon-phenolic heat shield or on the primary sandwich-type structure.

The aft heat shield is non-structural except for its own inertia loads. It consists of a hemispherical fiberglass honeycomb sandwich 0.6 cm (.25 in.) thick (two .012 in. fiberglass facesheets) to which is bonded a 0.25 in. thick open honeycomb core. The core is filled with a low density elastomeric ablator by vacuum techniques. The external appearance of the assembled probe is striking. The forward cone section is smooth dull black, while the aft dome is flat white finely detailed by the 0.25 in. honeycomb cell pattern. The afterbody is transparent to radio frequency energy for data transmission and is below 2.5 gm/cm^2 equivalent mass density to facilitate sensing of trapped particle radiation internally.

The probe mass properties requirements are.

- The center of gravity (C.G.) should be as far forward as possible and on the roll axis. Tests indicate C.G positions progressively greater than two percent aft of the theoretical diameter, i.e., aft of the intercept plane formed by extending the forebody/afterbody surfaces causes an increasingly unstable aerodynamic configuration.
- The roll inertia must be large relative to the pitch or yaw inertia; ratios greater than 1.2 1 are acceptable.
- The principal axis must coincide with the roll axis. All cross-products and C.G. eccentricities must be nulled to provide a known attitude at the beginning of entry.

A goal of the design activity has been to make a Jupiter entry probe that is of the order of 150 kg. The data of Figure 11 demonstrate that such a goal is realizable. Of particular significance is the fact that the science payload

MASS PROPERTIES

OPP-17

SUBSYSTEM	MASS (kg)
STRUCTURE	13 3
HEAT SHIELDS	68 6
HEATERS & INSULATION	6 9
COMMUNICATIONS & DATA HANDLING	10 3
ELECTRICAL POWER	9 3
PYROTECHNICS	3 7
SCIENCE PAYLOAD	20 4
INSTRUMENTATION	0 7
WEIGHT MARGIN (10%)	13 3
PROBE WEIGHT	146 5
LESS	
INTERFACE WIRING	-1 1
EXTERNAL INSULATION	-2 6
AT ENTRY	142 8
LESS ABLATION MATERIAL	-42 0
END OF MISSION	100 8
C G & INERTIAS AT ENTRY	
X AXIS C G * (PERCENT)	0 35
I_X (ROLL) gm-cm^2/10,000	11,262
I_Y (PITCH) gm-cm^2/10,000	6,884
I_Z (YAW) gm-cm^2/10,000	6,833

*EXPRESSED AS PERCENT OF DIAMETER AFT OF THE CONICAL FOREBODY AND THE SPHERICAL AFTERBODY

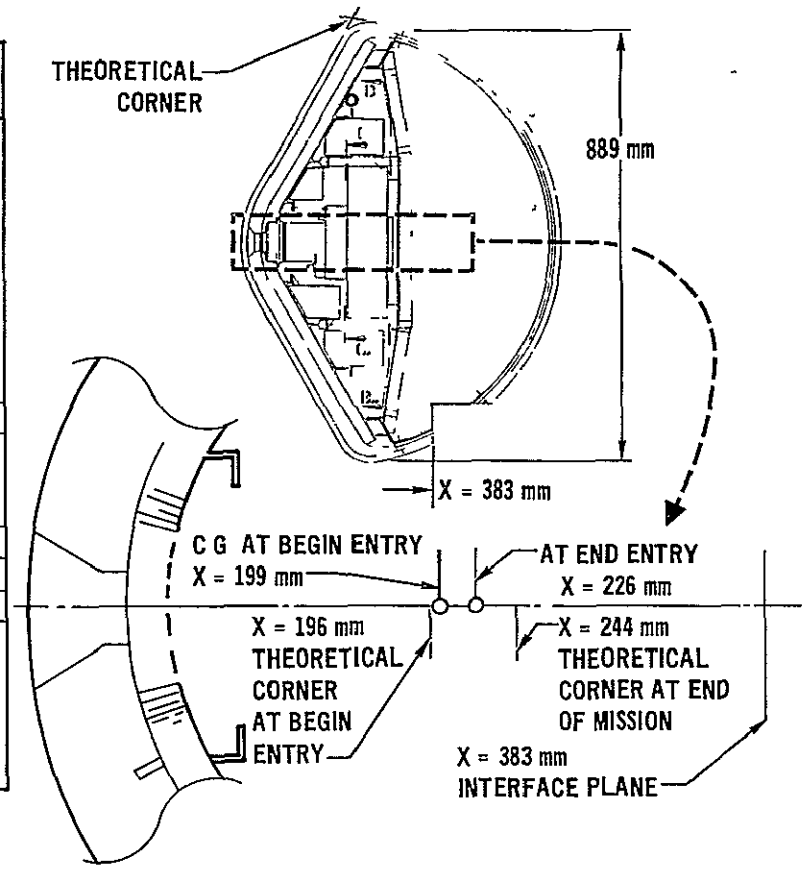

Figure 11

represents 14 percent of the take-off weight (20 percent of the end of the mission.) This has been achieved through careful design of the heat shield and restriction of the communications power level.

The probe internal equipment is packaged in toroidal segments that fit between the integrally machined rings. The equipment is attached to the rings by simple lug fasteners. The purpose of tailored equipment packaging is to keep the probe center of gravity forward, to provide uniform load distribution, and to achieve a I_{roll}/I_{pitch} ratio of 1.65. These factors increase aerodynamic static and dynamic stability and pre-entry spin-stability. They also assist in maintaining uniform internal temperature distributions. The toroidal arrangement includes circumferential wiring and peripheral connectors. The entire equipment section is enclosed by a foam-insulated cover that is

attached to the outer structural box ring and supported in the center by 3 bipod fittings that bear on the inner rings. A disc-shaped (34.3 cm dia. x .32 cm thick) micro-strip antenna is supported on the equipment cover under the 2.54 cm foam insulation. The antenna has an unrestricted beam width of more than 90 degrees through the aft hemispherical heatshield.

The aft heatshield has an access door for arming the probe's pyrotechnic systems and two jettisonable ports for science instrument viewing and deployment. The ports are jettisoned by compressed spring energy initiated by pyrotechnic bolt cutters. The aft heat shield has a small hole for passage of the probe-to-spacecraft umbilical. This umbilical is severed close to the surface of the probe by a spacecraft-adapter-mounted, pyrotechnic cutter just prior to probe release.

The probe internal temperature control is a semi-passive system. While the probe is attached to the spacecraft,internal temperatures are maintained by thermal conduction of radioisotope heater output to the three spacecraft adapter attach points. Temperature sensors, located on the spacecraft adapter, control the heaters on the adapter when temperature regulation is required. After separation the internal temperature is maintained between acceptable equipment limits by calculated heat balance between the internally generated heat from radio-isotope heater units (RHU's of 1 watt each) and conductive/ radiative losses through the probe structure and an external multilayer insulation blanket. The external blanket is made of 25 layers of goldized mylar separated by insulative plastic-net separators. The blanket is nominally 1.27 cm (.50 in) thick. The insulation is tuned or adjusted in transmissibility before flight by removing partial patches that are built into the outer layers of the insulation.

The configuration for probe stowage on the Pioneer spacecraft is on its shadowed side. Probe release from the spacecraft is by simultaneous gas activation of 3 ball-lock release devices. Separation is accomplished by 3 ball-lock release devices. Separation is accomplihed by 3 matched springs mounted concentrically with these release fittings. The three springs impart a 0.5 m/sec relative separation velocity. Once released the probe functions fully autonomously; the spacecraft initiates the deflection maneuver after a

timed interval that ensures adequate physical clearance of the probe as listed in Figure 5. Premature firing of deflection thrust chambers could alter the probe's attitude even though it is rotating at five revolutions per minute. This spin-rate is the nominal spin-rate for the Pioneer spacecraft but is a satisfactory balance between high rates to get uniform ablation and low rates to aid rapid tip-over in the atmosphere.

SCIENCE INSTRUMENTS

The primary function of the probe is to collect and transmit data that aids in characterizing the atmosphere of Jupiter. To date, all knowledge of Jupiter has been obtained remotely. However, even the close-up measurements of Pioneer 10 are not in agreement; for example, atmospheric temperatures derived from the infrared radiometer data conflict with the temperature profiles obtained by radio occultation By obtaining absolute measurements of temperature and pressure and correlating these with existing data, in situ measurements will enhance our understanding of some of the planetary atmosphere processes. In addition the accelerometer experiment provides atmospheric density measurement throughout the entry mission. As the probe enters the atmosphere, an onboard accelerometer senses a threshold, in this case ($-0.0004\ g_E$); the data handling system continues to record deceleration values at moderate rates until the deceleration peak occurs. This is defined as $a = -0\ 01\ g_E$ (axially) on the ascending side of the peak, and this serves as the rate-change cue. Because this specific value cues several probe functions, the accelerometer is backed up by a g-switch. Subsequently, other deceleration cues trigger other functions such as instrument deployment and radio transmission. This sequence of events is correlated with time and altitude and the usually defined cloud layers in Figure 12.

To characterize the atmosphere, the probe must carry a complement of instruments that can obtain a variety of data that permits correlation of Earth-bound and spacecraft-borne measurements. The complement of instruments is designed to fulfill the following objectives.

Near Planetary Radiation Environment - The energetic particle detector provides an integrated measurement of high-energy protons and electrons from 2 R_J to 1 R_J, to aid in completing the mapping of the Jovian radiation environment

Atmospheric Structure - The accelerometer experiment measures the aerodynamically-induced deceleration of the entry probe by the planetary atmosphere. The ambient atmospheric density is derived by computation from the aerodynamic deceleration readings. In the lower atmosphere the data on atmospheric structure from the accelerometer are supplmented by direct measurements of atmospheric temperature and pressure.

The location of cloud layers within the atmosphere is to be determined with a backscatter nephelometer. Information on the density of the layers and their optical opacity is obtained by combining a comparison of nephelometer and flux meter data which is measured in visible and infrared regimes.

OPP-1

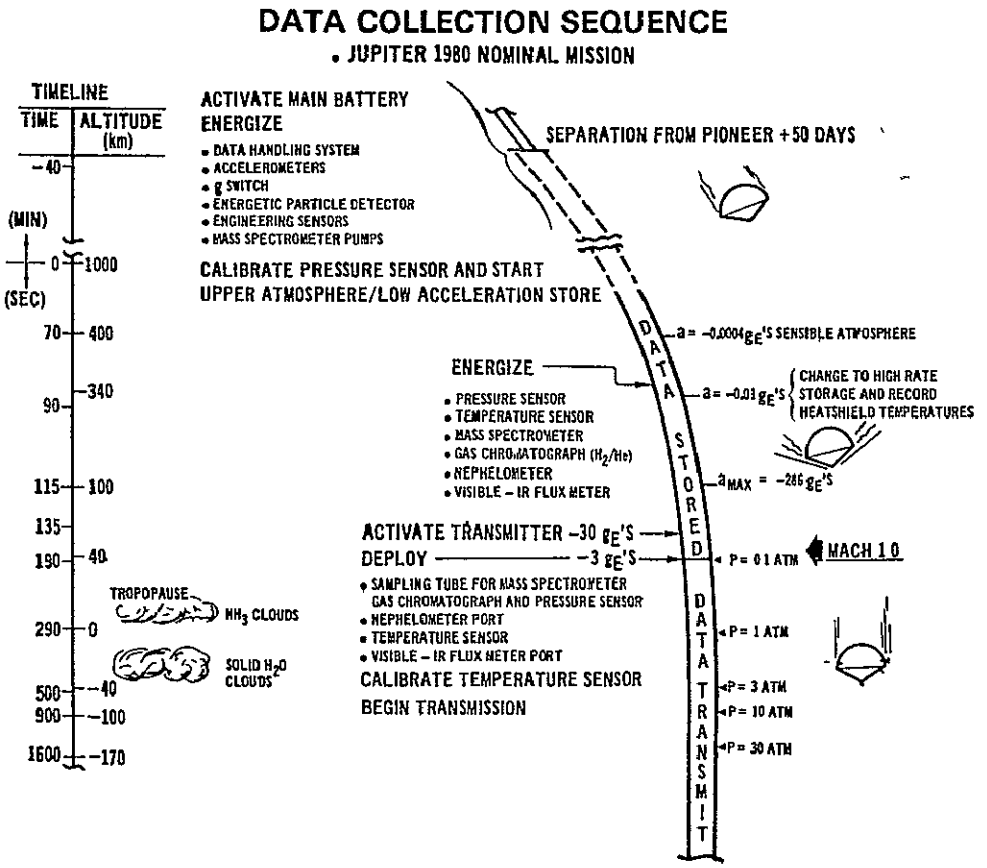

Figure 12

Atmospheric Composition - The chemical composition of the atmosphere is determined primarily by the mass spectrometer. A supplementary measurement of the hydrogen/helium ratio is provided by an explicitly designed gas chromatograph.

Radiation Balance - The thermal energy balance within the atmosphere is measured by the visible-infrared flux meter. These measurements are correlatable with those obtained on the orbiter.

Figure 13 lists the science instruments and measurement characteristics of each of these instruments.

Accelerometer - The accelerometer unit is a self-contained package that consists of three orthogonally mounted mass-rebalancing accelerometers along with their supporting electronics. It is a modified version of one used on the PAET vehicle and Pioneer Venus. The package is mounted with the longitudinal accelerometer aligned with the centerline of the probe and

with the proof mass as close as possible to the probe's center of gravity. A compromise location longitudinally is planned between fore-and-aft C.G. extremes.

SCIENCE PAYLOAD

OPP-22

INSTRUMENT	OBJECTIVES	RANGE	SAMPLE RATE
• ACCELEROMETER	DENSITY PROFILE	0 TO 0 1 g_E	1 sps DURING – 0 004 g_E TO –0 01 g_E
LONGITUDINAL		0 TO 10 g_E	
		0 TO 800 g_E	4 sps DURING – 0 01 g_E TO –3 g_E
LATERAL		0 TO 10 g_E	0 05 sps
• PRESSURE GAGE	PRESSURE PROFILE	0 TO 0 1 atm 0 TO 5 atm 0 TO 10 atm 0 TO 25 atm 0 TO 50 atm	0 05 sps (LOWER ATMOSPHERE)
• TEMPERATURE GAGE	TEMPERATURE PROFILE	50 TO 550°K	0 05 sps (LOWER ATMOSPHERE)
• NEUTRAL MASS SPECTROMETER	COMPOSITION	0 TO 40 AMU	CONTINUOUS SAMPLING WITHIN THE LOWER ATMOSPHERE (12 bps)
• GAS CHROMATOGRAPH	H_2/He RATIO	N/A	3 GAS SAMPLES (0 5 bps)
• VISIBLE/IR FLUX METER	TEMPERATURE VARIATIONS	0 5 TO 55 μm	3 0 bps
• NEPHELOMETER	CLOUD LAYERS	N/A	1 5 bps
• ENERGETIC PARTICLE	ENERGETIC PROTONS	PROTONS > 60 MeV	2000 bits

N/A = NOT APPLICABLE

Figure 13

Pressure Gage - The pressure gage is a single unit that contains four pressure transducers and a common electronics package. The inlet ports of the pressure gage is collocated within the mass spectrometer inlet probe assembly. The four transducers successively provide readings in the ever increasing pressure domains.

Temperature Gage - The temperature gage consists of two components, the deployable sensor unit and the electronics package. It is typical of platinum wire sensors used in many space probes except for its deployment. A mechanism is needed which must eject a carbon-phenolic plug. It is located outward on the forward cone to assure high velocity flow over the dual platinum wires.

Neutral Mass Spectrometer - The neutral mass spectrometer is a double focusing magnetic deflection instrument similar to one used on the

Atmospheric Explorer Satellite. Atmospheric gas samples are obtained through a 0.48 cm diameter tube which is concentrically housed within a deployable tube of 1.7 cm diameter. Deployment is initiated by a phrotechnic pin-puller which releases a preloaded metal bellows. A continuous sample of the atmosphere is tapped off a plenum via a sampling tube. As the probe descends thru the atmosphere, data is obtained at each pressure level. The continuous sampling spectrometer being considered required repackaging.

Gas Chromatograph (H_2/He Ratio) - The gas chromatograph shown is a modified version of the one being developed for the Pioneer Venus. This is a dedicated instrument which explicitly measures the H_2/He ratio during the probe descent. It also taps off of the plenum and is a single column instrument.

Visible Infrared Flux Meter - The visible-IR flux meter is an adaptation of the Pioneer Venus net flux radiometer. The instrument is deployed by a spring loaded four bar mechanism through a jettisonable port in the aft heat-shield. The detector looks down at the planet to measure variation in radiant energy levels as the probe descends into the atmosphere. An upward measurement is of little value as the current entry longitude is 15-20 degrees beyond the evening terminator.

Nephelometer - The nephelometer is a Ames Research Center design for the Pioneer Venus probe. The instrument consists of a light source, lenses and an optical detector. These components together with the power supply and data processing electronics are packaged into a single unit. The unit is located aft of the foam equipment cover and looks out radially after porthole cover removal. The incident light on a particle produces backscattered light which is simply tallied for relative transmission. No sizing of particles is accomplished.

Energetic Particle Detector - The concept of the energetic particle detector is based on the Aerospace Corporation detector used on ATS 1. Modifications to the packaging are required to fit it into the probe. The detector looks aft thru the probe aft heat shield with a 40° cone-angle field of view. The detector measures energetic protons above 60 Mev and a spectrum of electrons. The instrument will function during the 45 minute period of descent that

precedes entry. It is energized on a signal from the x-day clock, which also energizes the data handling system and its special store.

Each of the instruments are accommodated within the probe as shown in Figure 14. Addition of a gas chromatograph and a energetic particle to the science payload necessitated a rearrangement of some toroidal segments and relocation of some connectors within the baseline design. The visible-infrared flux meter is located in the aft hemisphere. It requires the incorporation of a new porthole in the aft heat shield, but little else besides thermal insulation. Two science instrument changes also resulted from the rearrangements: the temperature sensor is mounted radially farther out as are the pressure sensor capsules.

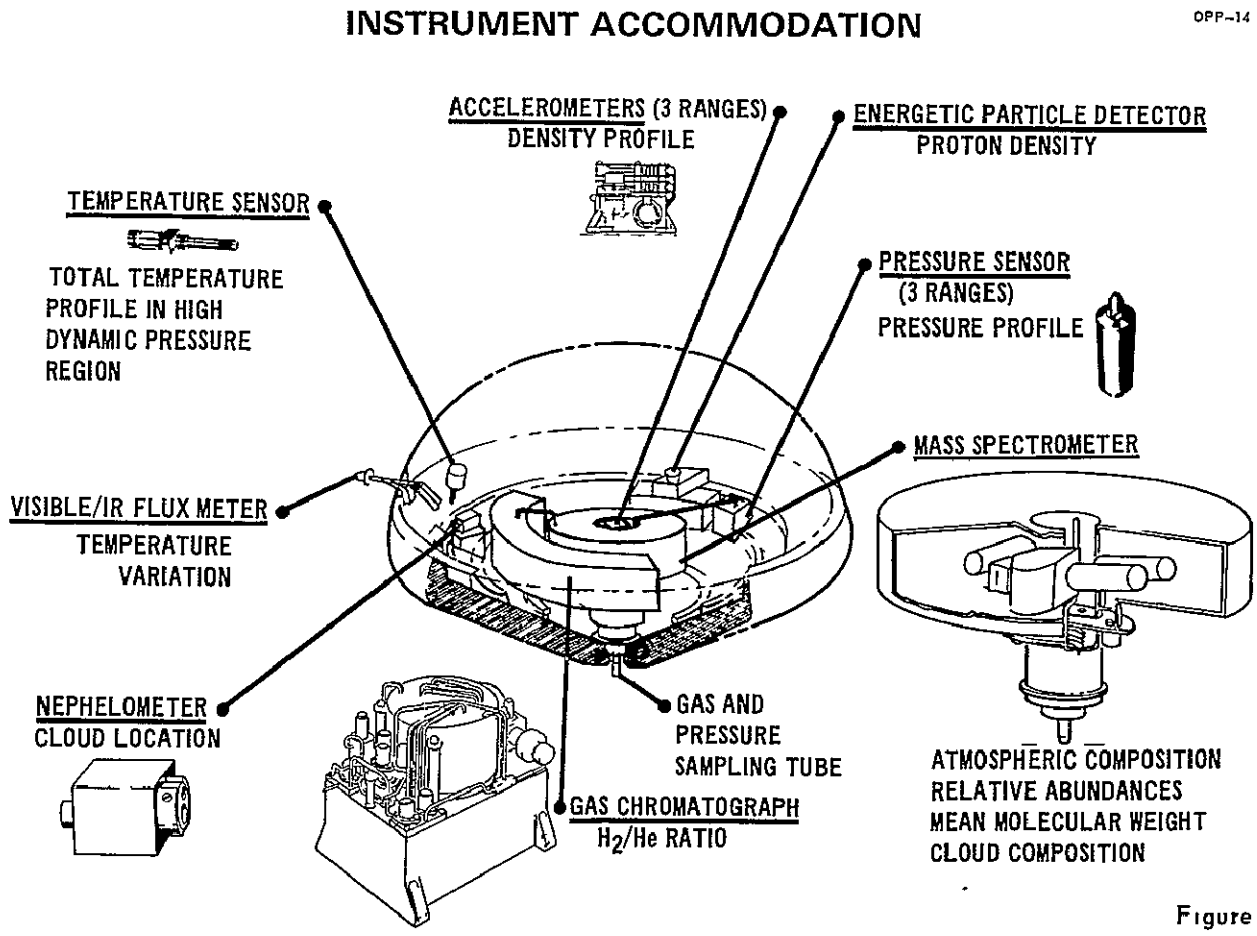

Figure 14

The post-entry science data formats are revised from the SUAEP design to accommodate the addition of the gas chromatograph and the visible-infrared flux meter. Two are shown in Figure 15, one of which includes rates recommended by Ames Research

Center (design A) and an alternate (design B) which simplifies data handling and minimizes the post entry data rate, thus allowing the redundant dumping of the preentry store. The problem of formatting is to assemble the data requirements into an integer mathematical structure which provides the appropriate sampling intervals for each instrument, and can be decommutated - the addition of a synchronization word. The format diagrams below the table in Figure 15 illustrate the mathematical structures of the formats. In designs A, the 10 bit science words are bit summed (interleaved) with the continuous neutral mass spectrometer bitstream and the 6 bit engineering words. In design B, the continuous rate neutral mass spectrometer data (cut from 12 BPS to 2 BPS by transmitting only the peaks of the data) is broken into 10 bit segments and formatted with the other post entry science and, then, bit summed with the engineering as before. The complete data handling system is shown in Figure 20, with the preentry data dump.

POST ENTRY SCIENCE DATA HANDLING*

OPP-6

INSTRUMENT	BIT RATE		
	DESIGN A1	DESIGN A2	DESIGN B
NEUTRAL MASS SPECTROMETER (NMS)	12 0	12 0	2 0
GAS CHROMATOGRAPH (GC)	0 5	0 5	0 4
PRESSURE (P)	0 5	0 5	0 2
TEMPERATURE (T)	0 5	0 5	0 2
ACCELERATION (X)	0 5	0 5	0 2
(Y)	0.5	0 5	0 2
(Z)	0 5	0 5	0 2
RADIOMETER (R)	3 0	2 0	2 0
NEPHELOMETER (N)	1 5	2 0	2.0

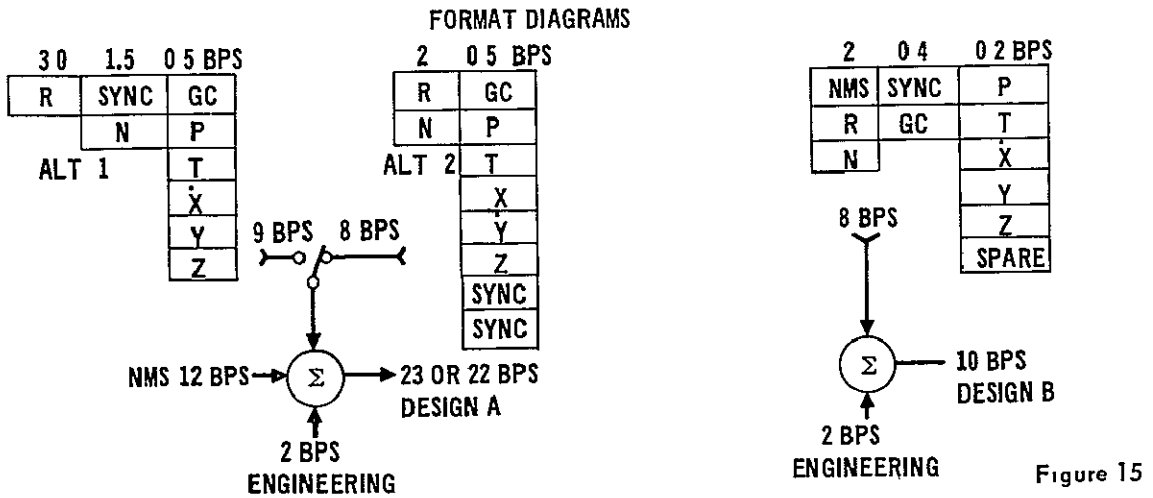

Figure 15

*SEE FIGURE 20 FOR DATA HANDLING SYSTEM WITH PREENTRY DUMP

The probe design now accommodates 20.4 kg of scientific instruments, and an increased engineering instrument complement as listed in Figure 16. Direct measurement of heatshield response to atmospheric heating in four forward heatshield and one aft heatshield location is included with previously required calibration and housekeeping information. All of the engineering sensors are sampled during preentry data storage and post entry, real-time transmission. These provisions will aid in data interpretation and, if needed, fault determination.

The engineering sensors could be cycled during interplanetary transit to check on probe status. The probe accelerometer can be used in all spacecraft maneuvers for comparison with spacecraft motion for performance checks of the acclerometer. However, merit is also seen in leaving the probe completely dormant during all post launch activities (except Ni-Cd battery discharge-recharge cycling) to avoid use degradation.

OPP-36

ENGINEERING MEASUREMENT LIST

PARAMETER	INPUT VOLTAGE RANGE (VDC)	TYPE	QUANTIZATION	SAMPLE RATE (SPS)
FORWARD HEATSHIELD SENSOR 1	0–40mV	DELL[1]	6	5 & 1
FORWARD HEATSHIELD SENSOR 2	0–40mV	DELL	6	5 & 1
FORWARD HEATSHIELD SENSOR 3	0–40mV	DELL	6	5 & 1
FORWARD HEATSHIELD SENSOR 4	0–40mV	DELL	6	5 & 1
AFT HEATSHIELD SENSOR	0–40mV	DELL	6	5 & 1
HEATSHIELD TEMPERATURE NO 1	0–5	SEHL[2]	6	5/6 & 1/336
HEATSHIELD TEMPERATURE NO 2	0–5	SEHL	6	5/6 & 1/336
HEATSHIELD TEMPERATURE NO 3	0–5	SEHL	6	5/6 & 1/336
AFT SHIELD TEMPERATURE NO 1	0–5	SEHL	6	5/6 & 1/336
AFT SHIELD TEMPERATURE NO 2	0–5	SEHL	6	5/6 & 1/336
ACCELEROMETER TEMPERATURE	0–5	SEHL	6	5/6 & 1/42
PRESSURE GAGE TEMPERATURE	0–5	SEHL	6	1/42
TRANSMITTER CRYSTAL TEMPERATURE	0–5	SEHL	6	1/336
BATTERY TEMPERATURE	0–5	SEHL	6	1/42
DHS TEMPERATURE	0–5	SEHL	6	1/336
BATTERY VOLTAGE	0–5	SEHL	6	1/42
VOLTAGE STANDING WAVE RATIO (VSWR)	0–5	SEHL	6	1/42
TRANSMITTER POWER	0–5	SEHL	6	1/42
RELATIVE TIME (INTERNALLY GENERATED)			12 BIT WORD	1/42
ACCELEROMETER RANGE – CHANGE NO 1	0–5	BL[3]	ONE 6 BIT WORD	ON OCCURRENCE
ACCELEROMETER RANGE – CHANGE NO 2	0–5	BL	ONE 6 BIT WORD	ON OCCURRENCE
G-SWITCH ACTUATION	0–5	BL	ONE 6 BIT WORD	ON OCCURRENCE
PYRO RELAY STATE	0–5	BL	ONE 6 BIT WORD	ON OCCURRENCE

1 DELL DOUBLE ENDED LOW LEVEL
2 SEHL – SINGLE ENDED HIGH LEVEL
3 BL – BILEVEL
IN ADDITION, INTERNAL INSTRUMENT CONDITION DATA ARE CONTAINED IN ITS DATA STREAM

Figure 16

SUBSYSTEM DESIGN

The subsystems of the entry probe have all been reexamined to assure compatibility with the objectives and requirements of a Pioneer Jupiter Orbiter Probe flight in 1980. The subsystem most affected by the mission is communications. The lower signal-to-noise ratio and the geometry necessitate increasing power to a 60W level relative to SUAEP design. The heat protection subsystem is slightly changed from earlier Jovian entry studies. Refinements in analysis and the accumulation of data, (that the real atmosphere lies near Nominal and Warm models) leads to the conclusion that modest reductions in protection can be effected. The science and engineering instrument additions coupled with a transmitter power increase consumes more of the energy provided than that previously reported upon. Thermal studies indicate that temperatures rise at a faster rate but, as yet, not critically in the short duration Jupiter descents. The pyrotechnics will change when the continuous flow neutral mass spectrometer is completely accommodated. This report continues to illustrate the batch type, because a repackaging study is incomplete, but the analysis and data rates are based on the continuous form.

Telecommunications - The telecommunications subsystem is redesigned, based on the Ames Research Center trajectories in the following table, and the recommended Outer Planets Probe Science Advisor Group science payload is shown in Figure 13. Details of the analysis of this design are contained in Reference (a). The design proceeds in three steps: first, the missions (trajectories), antenna patterns and carrier frequency are parametrically investigated to determine the optimum mission/radio characteristics. Second, the science payload requirements together with the engineering (housekeeping) requirements are formulated into detailed data handling systems. Finally, the combinations of the radio and data systems are evaluated to define an optimal telecommunications system.

The starting point for the communications subsystem design is the relative trajectories of the spacecraft and the probe, from entry to 30 minutes after entry, where the probe is at either the 30 bar level (for the Nominal atmospheric model) or at the 22 bar level (for the Warm atmospheric model). The end points of the three trajectories investigated are tabulated below. In addition to these trajectories (Options A, B, & C), a fourth trajectory was supplied (Option D) too late for analysis.

END POINT GEOMETRIES FOR OPTIONAL ARC TRAJECTORIES

Mission Option	Parameter*	Entry (t=0)	End of Mission (t=0.5 hr)
A	1	40.8	11.7
	2	49.5	96.7
	3	76,674	58,541
B	1	41.5	17.5
	2	48.2	92.6
	3	81,375	63,143
C	1	43.0	15.9
	2	46.8	95.1
	3	77,644	58,671
D	1	40.4	13.0
	2	49.4	99.4
	3	75,200	58,400

*Condition 1 Probe Angle - degrees
2 Spacecraft Angle - degrees
3 Transmission Range - km

The Options B and C are baselines that direct the spacecraft to a nearly equatorial Jovian plane. Option A is for the spacecraft in the plane of probe entry. In the latter stages of the telecommunications design, after Option A had been selected for study, Ames Research Center formulated another equatorial spacecraft plane trajectory with similar communications geometry. This is Option D. Figure 17 illustrates the relative geometry of the Option A mission.

OPP-5

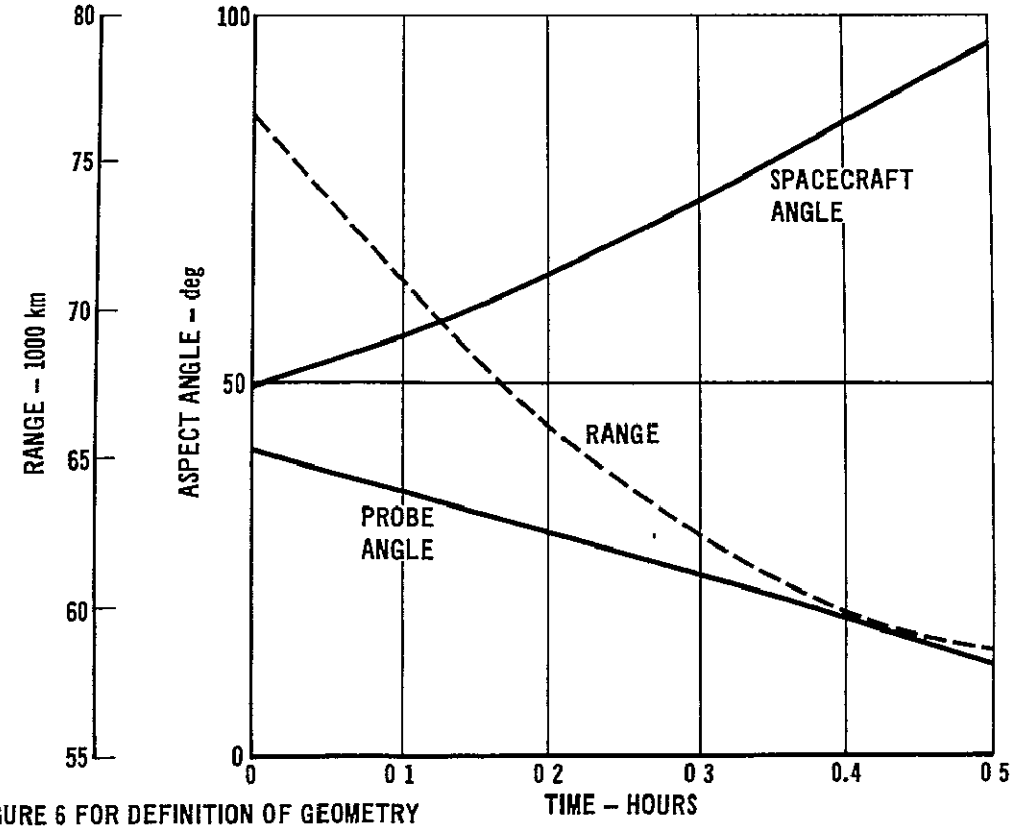

*SEE FIGURE 6 FOR DEFINITION OF GEOMETRY

Figure 17

The first step in the design investigates the effects of carrier frequency. From the NASA SP8069,defining the environment of Jupiter,it is readily seen that planet noise and synchrotron noise as well as ionospheric loss and antenna size favor high frequencies, while atmospheric loss and free space loss favor lower frequencies. A parametric study from 400 to 1000 megahertz (MHz) indicated a fairly broad null about 400 megahertz with probe beamwidths between 66 and 114 degrees. Given the carrier frequency, a three dimensional tradeoff of probe beamwidth, spacecraft beamwidth and spacecraft beamcenter was conducted. Figure 18 is illustrative of the analyses. For a given probe beamwidth and spacecraft beamwidth-beamcenter the optimal (minimum) transmitter power is required where the power at the initial portion of the mission equals the power at the end of the mission. In both cases the new angle is off of the peak gain angle. For the three missions investigated, for probe beamwidths from 66 (aperture limit) to 114 degrees, for spacecraft beamwidths from 40 (physical size limitation) to 70 degrees and for spacecraft beamcenters from 35 to 70 degrees; the optimal combination for minimum power per bit is 64/44 watts/bit for a 66 degree probe beamwidth and a 50 degree spacecraft beamwidth at a 56 degree beamcenter.

OPP-23

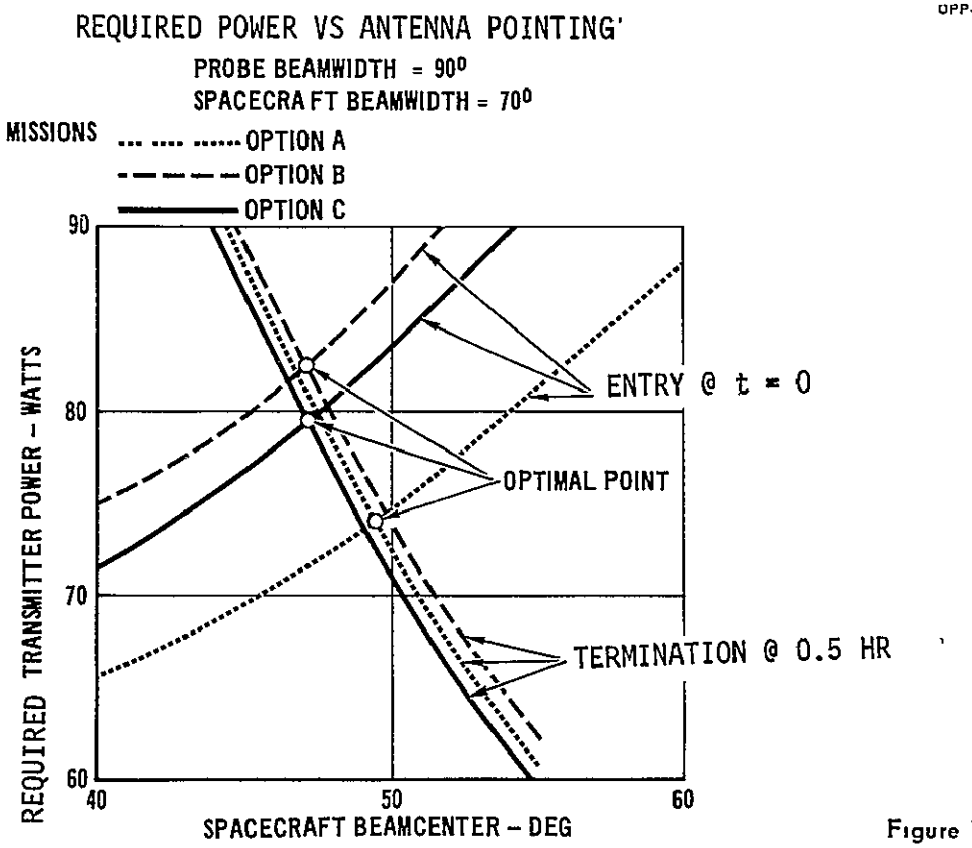

Figure 18

The scientific data requirements are summarized in Figure 13. From the data handling system viewpoint the requirements can be broken into two portions. First there is the preentry portion (radiation measurements and high rate deceleration) when transmission is not available due to unfavorable aspect angles and entry plasma blackout. Data from this portion of the mission is stored. High rate engineering heat shield information is also desirable in this portion of the mission. Second, there is the post entry science portion during which the stored preentry information must also be transmitted.

The preentry (actually pretransmission) data can be accommodated by a 2000 bit radiation store, a 14,736 bit deceleration store and a 6092 bit heat shield store. Three alternatives were investigated for the post entry real time data.

POST ENTRY FORMATS

Instrument	Design A1	Design A2	Design A3
Neutral Mass Spectrometer	12 bps	12 bps	2 bps
Gas Chromatograph	.5 bps	.5 bps	.4 bps
Visible-IR Flux Radiometer	3 bps	2 bps	2 bps
Nephelometer	1.5 bps	2 bps	2 bps
Other Science (p, T, g)	.5 bps	.5 bps	.2 bps
Engineering Rate	2 bps	2 bps	2 bps
Total Post Entry Rate	23 bps	22 bps	10 bps

The essential differences between the designs are that Designs A1 and A2 have a continuously sampled neutral mass spectrometer (12 bps) vs Design B which only transmits the spectrometer peaks (2 bps), and that the other science (pressure, temperature and accelerations) in designs A1 and A2 are 0.5 bps vs 0.2 bps in design B.

At this point a radio system has evolved (64 watts/44 bps), a preentry store sized (22,828 bits) and three post entry real-time rates conceived (10, 22 and 23 bps). The remaining task is to marry the designs. Essentially, this means reading out the preentry store together with the post entry real-time data and sizing the transmitter. Figure 19 illustrates the trade. It is seen that the combinations of readout rates and real-time rates are bounded on one side by transmitter size in the current state of the art and on the other by the inability of the system to totally dump the preentry store. Considering that the 60 watt 400 megahertz state-of-the-art bound is "soft", i.e., a slight link penalty may be acceptable, whereas, a minimum readout of the preentry store is a "hard" limit, acceptable systems range from the 24 bps design. The 23 bps design is artificially increased to 24 bps to facilitate interleaving by increasing the post entry sampling rates by 10/9.

at a 4:3 interleave to a 10 bps design with 2:3 to 1:3 interleave with a real time/delay time. Because a 12 bps neutral mass spectrometer (24 or 22 bps design) provides more constituency data, the 2 bps spectrometer (10 bps design) was not considered further. A reasonable choice, with simple interleaving is the 22 bps real-time 1:1 interleave. For a 60 watt transmitter this imposes only a -0.28 dB link penalty.

DATA HANDLING SYSTEM SELECTION

REAL TIME SYSTEM	PARAMETER	REAL TIME STORE INTERLEAVING 4 3	1 1	2 3	1 2	2 5	1 3
24 PBS (23 BPS DESIGN X24/23 SPS)	1	18 0	24.0	36			
	2	42 0	48 0	60			
	3	1 23	1.64	2 46			
	4	61 09(S)	69 82(S)	87.27(S)			
	5	– 0 08	–0 66	–1 63			
22 BPS	1	16.5	22 0	33 0	44 0	55.0	
	2	38 5	44 0	55 0	66 0	77.0	
	3	1 13	1 50	2 26	3 01	3 76	
	4	56 0	64 0 (S)	80.0 (S)	96 0 (S)	112 0 (S)	
	5	+0 30	–0 28	–1.25	–2 04	–2 71	
10 BPS	1	7 5	10 0	15.0	20.0	25 0	30.0
	2	17 5	20.0	25 0	30.0	35.0	40.0
	3	0 51 (U)	0 68 (U)	1 03	1.37	1.71	2.05
	4	25 45	29 09	36 36	43 64	50.91	58 18
	5	+3 72	+3 14	+2 18	+1.38	+0.71	+0 13

PARAMETER
1 PREENTRY PLAYBACK RATE, BPS
2 TRANSMITTED DATA RATE, BPS
3 NUMBER OF DUMPS IN 26 MIN = RATE X26X60/22828
4 TRANSMITTER POWER, WATTS, = RATE X64/44
5 60 WATT TRANSMITTER PENALTY/ADVANTAGE, dB

NOTES
(S) BEYOND THE STATE OF THE ART
(U) UNACCEPTABLE

Figure 19

The data handling functional block diagram is shown in Figure 20 with the readout of the stores in Figure 21. Prior to entry an onboard clock initiates the data system ON. From this point, nominally at 2 Jovian radii, the radiation sensor begins filling its 2000 bit store, and the acceleration processor monitors the longitudinal accelerometer for -0.01 g_E (meanwhile dumping the accelerometer data into a first-in last-out line). At -0.01 g_E (backed up by a g-switch) the accelerometer data between -0.0004 g_E and -0.01 g_E is trapped in this line and high sampling rate deceleration data is then stored. On sensing

-3 g_E on the down-side of the peak, the preentry processors are terminated. Next, the post entry processors and radio transmissions are initiated. As the receiver on the spacecraft must search in frequency for the probe signal (Doppler), a 2 minute delay line real-time acquisition store assures the first real-time data is then interleaved with the real-time data. The margin history for the link is given in Figure 22.

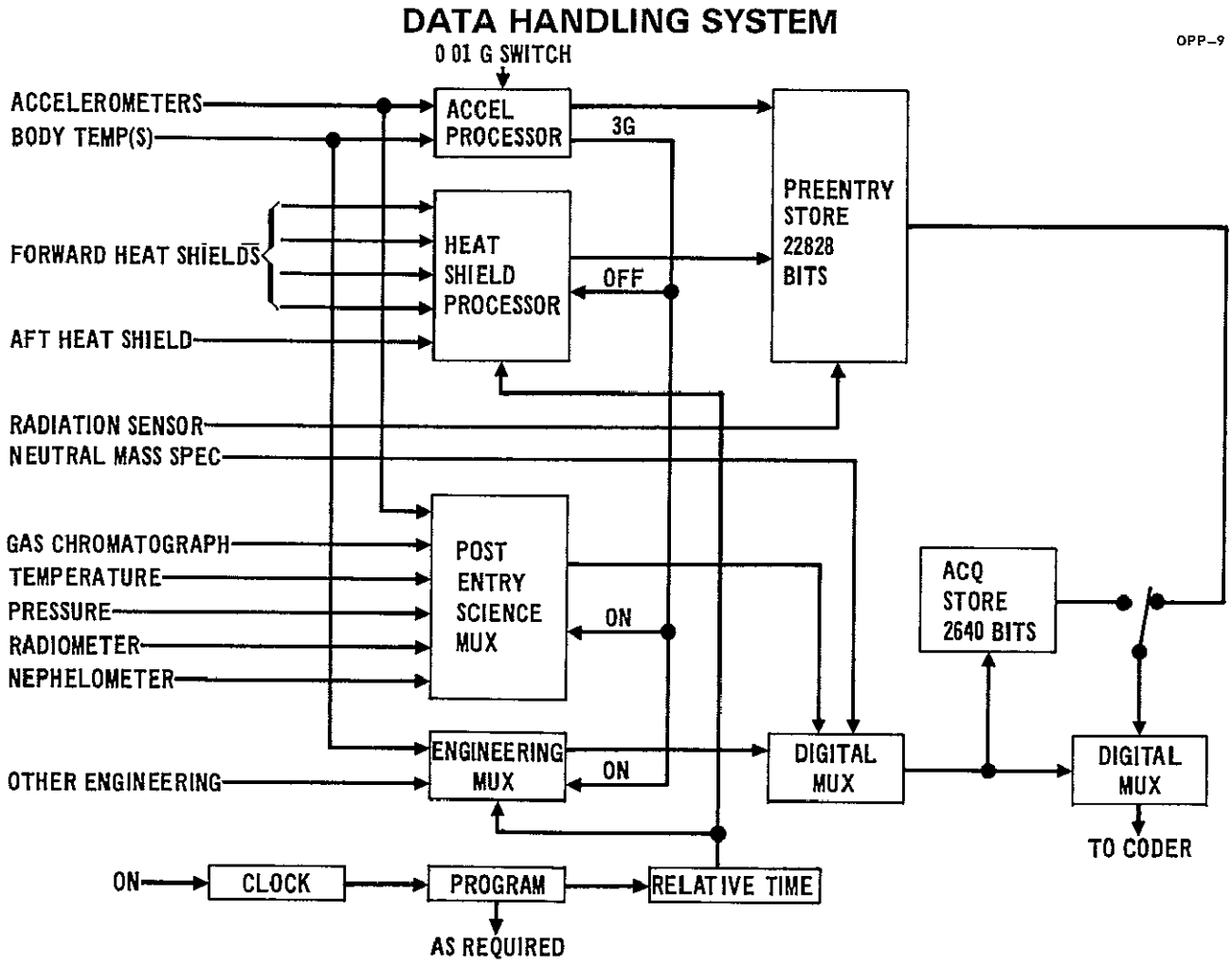

Figure 20

DATA STORAGE AND TRANSMISSION

OPP-18

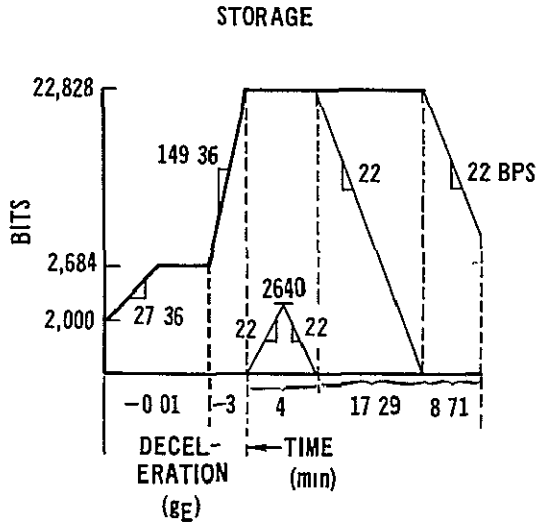

Figure 21

COMMUNICATIONS MARGIN HISTORY

OPP-4

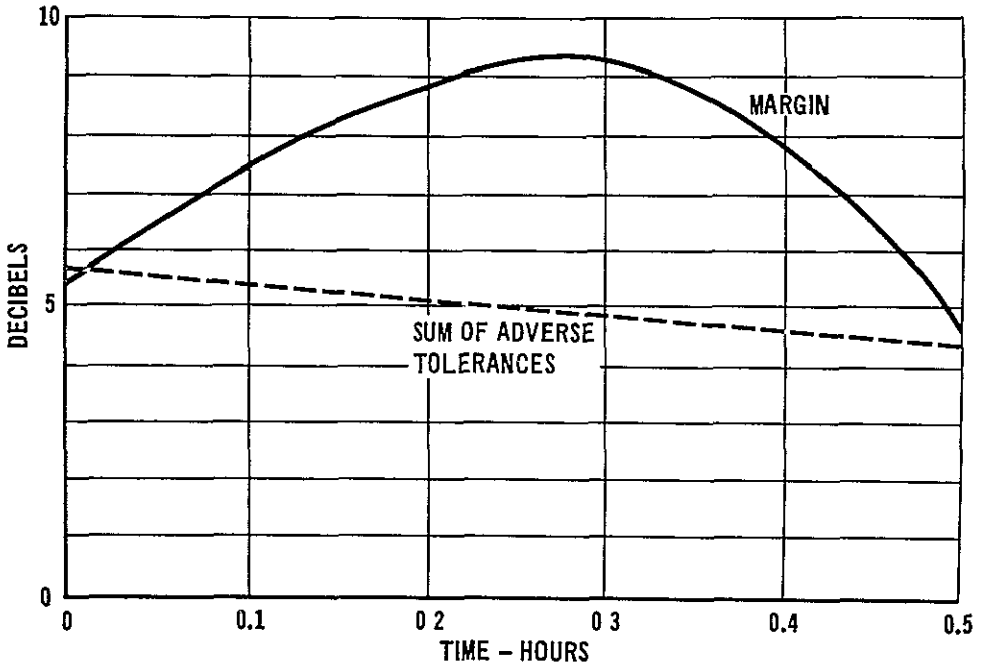

Figure 22

The telecommunications design is summarized in Figure 23. Included in the figure are two design alternatives which have not been fully explored. In the radio design an attractive alternative would be the use of two spacecraft antennas (actually one physical antenna with an electronic beam center switch). This probably would decrease the transmitter power by one-half. Such an antenna would be larger than a single beamcenter, and, hence, would physically benefit from higher frequencies. The Jovian noise environment is better known at the higher frequencies. If peak neutral mass spectrometer data only is adequate (rather than continuous samples), the 10 bps real-time rate which will definitely decrease the transmitter power required. This alternative to data collection deserves further study to ascertain the ability to reconstruct the atmosphere.

SUMMARY AND ALTERNATIVES

OPP-29

DESIGN SUMMARY

COMMUNICATIONS

- 400 MHz
- 44 BPS
- 60 WATT
- NONCOHENT TRANSMISSION
- CONVOLUTIONALLY CODED
- HARD DECISION DECODED
- 66^0 TRANSMIT ANTENNA
- 50^0 RECEIVE ANTENNA AT A 56^0 CONE ANGLE

DATA HANDLING

NEUTRAL MASS SPEC	= 12 BPS
POSTENTRY SCIENCE	= 8 BPS
ENGINEERING	= 2 BPS
PREENTRY PLAYBACK	= 22 BPS
TOTAL	= 44 BPS

STORAGE

RADIATION	= 2000 BITS
ACCELERATION	= 14,736 BITS
HEAT SHIELD	= 6092 BITS
ACQUISITION	= 2640 BITS
TOTAL	= 25468 BITS

DESIGN ALTERNATIVES

COMMUNICATIONS

INCREASE TOTAL RECEIVED POWER BY SWITCHING INFLIGHT BETWEEN TWO SPACECRAFT ANTENNA PATTERNS PROBABLY INCREASE CARRIER FREQUENCY TO 500 – 600 MHz TO REDUCE ANTENNA SIZE RESULT IN APPROXIMATELY 1/2 TRANSMITTER POWER

DATA HANDLING

REDUCE NMS RATE TO 2 BPS BY TRANSMITTING ONLY PEAK VALUES RATHER THAN CONTINUOUS ANALOG SAMPLES

- BIT RATE = 30 BPS
- OUTPUT INTERLEAVE = 1 2
- TRANSMITTER = 44 WATTS

Figure 23

Entry Heating and Heat Protection - Entry into Jupiter will impose a severe entry heating environment that must be dissipated by an efficient and reliable heat protection system. To reduce the magnitude of heating, it is desirable to enter the planet at a shallow angle (within the aiming uncertainties), to enter

near the equator (to obtain the maximum benefit of the planet's rotation) and to utilize a blunt configuration with low ballistic parameter (in order to decelerate at high altitudes). Figure 24 illustrates the heating and pressure environment associated with shallow entries for the three monograph models (NASA Report SP-8069) defined atmospheres. Preliminary analyses of the Pioneer 10 atmospheric structure experiments indicate an atmosphere model, at least in the high altitudes where heating actually occurs, that is very similar to the monograph defined Nominal Jupiter model. The combination of entering at shallow angles into an atmosphere that produces less severe heating than the Cool or the Nominal model has greatly alleviated the heating problem and makes the Jupiter mission within the realm of feasibility of state-of-the-art heat protection designs.

OPP-30

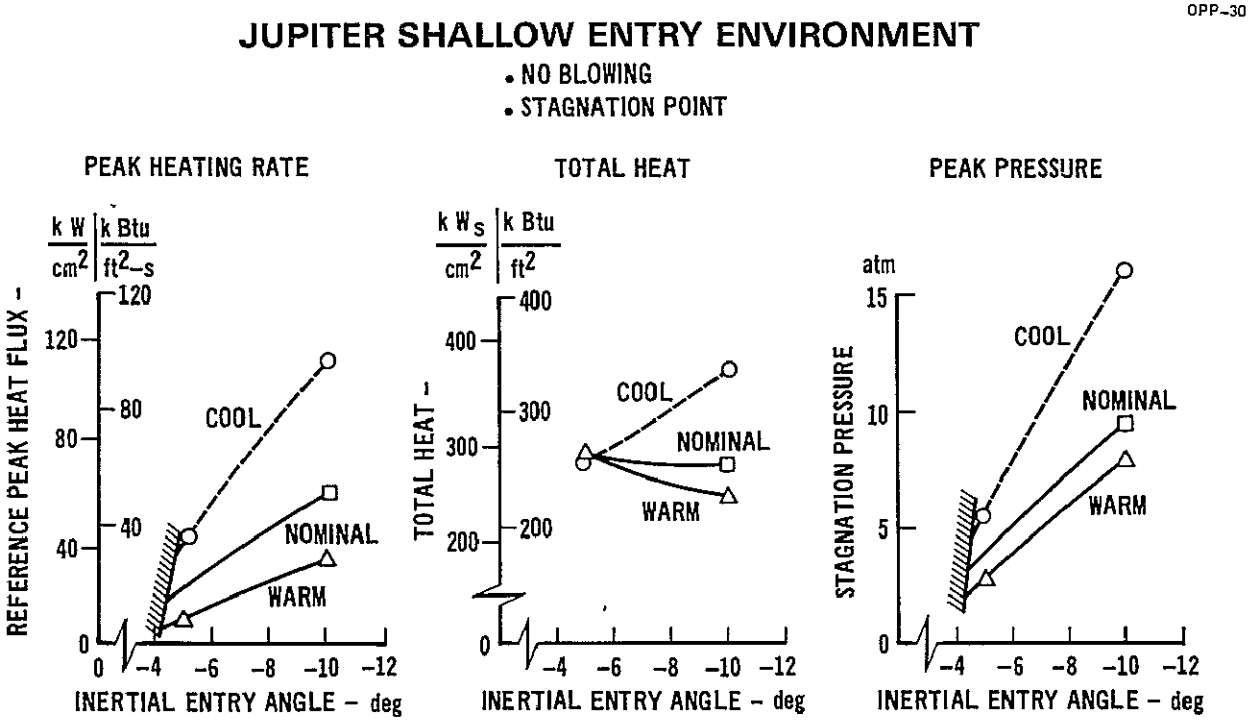

Figure 24

Figure 25 shows a comparison of the net heating and pressure histories expected for probe Jupiter entry with the environment encountered by a missile control surface (flap) protected with a carbon phenolic heat shield. The comparison is in terms of net heating reaching the surface, that is, the reduction in heating due to blowing has been accounted for. The main difference in the two environments is that the heat flux reaching the surface of an outer planet

probe is primarily radiative and the shock layer gas is a mixture of hydrogen/helium, whereas, in missile flights the heating is convective and the shock layer gas is oxygen-rich air. The difference in gas composition should have very little effect on material performance because the surface is in the sublimation regime during the high heating regime. This conclusion has been verified in available ground test facilities. The difference in material performance between a convective versus a radiative environment should be small since carbonaceous materials are opaque to radiation and absorb the incident radiative energy at the surface just as in the instance of convective heating. In other words, both forms of energy are absorbed on the surface and this energy is primarily dissipated by sublimation of the carbonaceous char. The rate of sublimation and the recession rate are dependent on the incident energy flux whether radiant or convective or both to the surface. Therefore, the probe heat shield that receives the higher energy flux, as shown in Figure 25, will

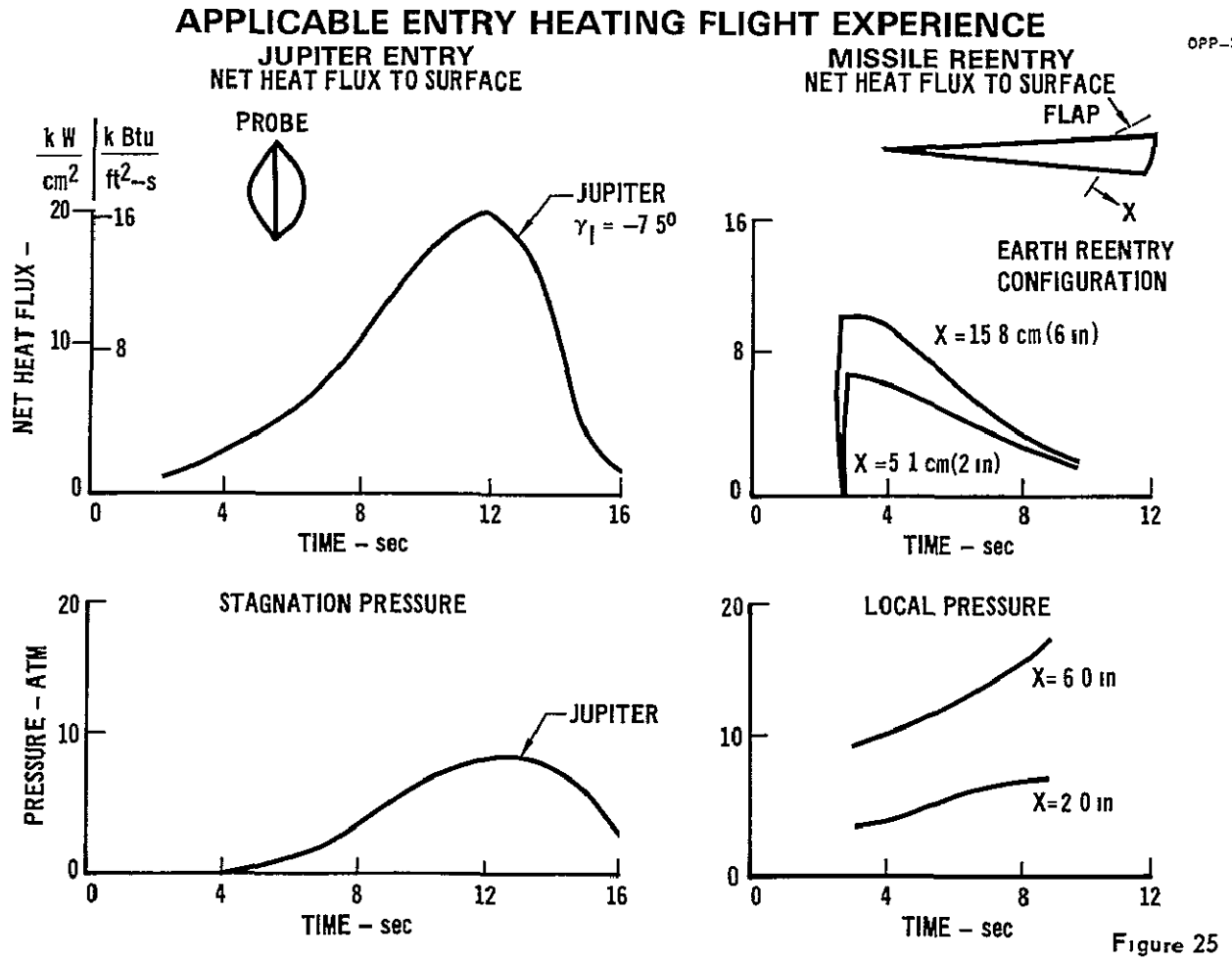

Figure 25

recede at a faster rate. On the other hand, the heat shield in both entry cases will attain similar surface sublimation temperatures. Note that entry surface pressures are similar. In both cases, the heat shield will have thin but similar char layer thickness due to the high recession rates. Therefore, both will experience steep, though similar, temperature gradients in the char which means similar char thicknesses and temperatures on both sides of the char layer. This similarity permits direct application of the missile flap technology data to validate the probe heat shield design at this stage of probe development.

Figure 26 presents the carbon phenolic heat shield thicknesses and weights needed to limit the fiberglass substructure face to 700K (800°F) maximum for the design value of entry angle (γ = -7.5 degrees). Because of the intense heating environment, a large portion of the initial thickness is consumed by sublimation (herein labeled thermochemical recession) and by mechanical erosion as estimated from missile flight data correlations. For the shallow entry envelope shown, about 35 to 45% of the probe weight must be allotted to heat protection.

CARBON PHENOLIC HEAT SHIELD REQUIREMENTS

OPP-32

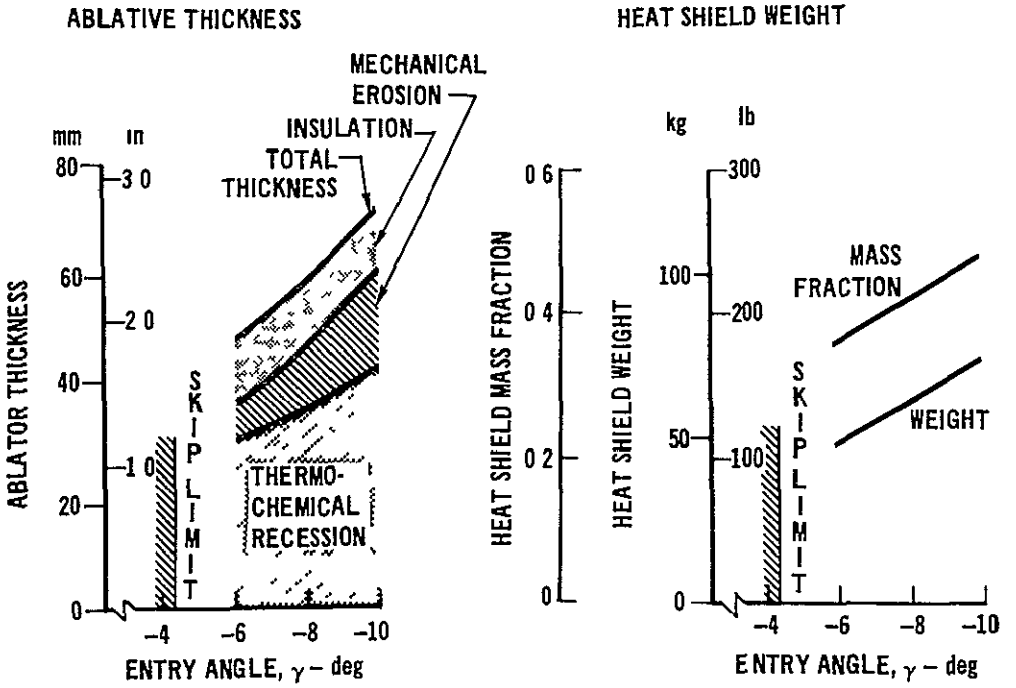

Figure 26

New advances in heat shield technology have been aimed at developing materials that reflect the incident shock layer radiation rather than absorbing it as do carbonaceous materials. A high density, high purity all-silica material appears to be the most promising reflective heat shield material and is currently under intense development. A characteristic of the reflective concept is that heat shield weights decrease with steeper entries, since a greater portion of the incident heating is radiative, thus the shallow entry constraint required for the carbon-phenolic heat shield may be modified if the reflective material achieves the good performance indicated by preliminary work. This achievement is sought because communications are enhanced by steep entries (γ > -7.5 degrees), whereas, heat protection thicknesses are decreased by shallow entries (-7.5 degree > γ > skip-out boundary).

Electrical Power - The electrical power/energy requirements for the Jupiter Orbiter Probe mission are tabulated in Figure 27. The tabulation identifies

EQUIPMENT POWER/ENERGY REQUIREMENTS

OPP-21

EQUIPMENT	UNIT POWER (WATTS)	TIME (MIN)	ENERGY (W-H)
ENTRY DETECTION			
X-DAY CLOCK (2)	140×10^{-6}	72,000	0 34
G-SWITCH	0 2	47	0 15
DATA HANDLING SUBSYSTEM	10 0	77	12 83
TRANSMITTER-OSE/MOD	1 0	77	1 28
POWER AMPLIFIER	135	30	67 00
SCIENCE			
MASS SPECTROMETER	11 0	40	7 33
GETTER PUMP HEATER	30 0	10	5 00
ORDNANCE RELAYS	3 0	0 001	0 05
GAS CHROMATOGRAPH	9 7	30	4 85
ACCELEROMETER	1 5	77	1 92
PRESSURE GAGE	1 2	30	0 60
TEMPERATURE GAGE	1 0	30	0 50
NEPHELOMETER	1 0	30	0 50
ENERGETIC PARTICLE DETECTOR	0 5	47	0 39
IR FLUX METER	3 0	30	1 50
ORDNANCE RELAYS	3 0	0 001	0 04
BATTERY HEATER	30 0	30	15 00
EQUIPMENT ENERGY			119 28
DISTRIBUTION LOSSES (5%)			5 96
TOTAL ENERGY REQUIRED			125 24

Figure 27

the individual equipment power requirements for the probe's subsystems. The energy users include entry detection, data handling, telecommunications, science payload, and the power subsystem (battery heaters). The operating times are derived from the mission timeline. The highest steady state power load is required during data transmission when the science and all engineering instruments, data handling and telecommunication subsystems are operating simultaneously. This electrical power load is 174 watts. With a data transmission time of up to 30 minutes, this phase consumes the major portion of the total energy.

The probe imposes an interfacing electrical energy requirement on the spacecraft during the interplanetary flight. The probe has a continual, low-wattage heat leak which the spacecraft modulates by direct control of the adapter temperature. A few watts are required to heat the Pioneer spacecraft probe adapter, but no electrical energy is expended as heat within the probe. This indirect method obviates the need for closed loop temperature control wiring across the interface. The other electrical energy requirement imposed is a need to charge (repeatedly) the nickel cadmium (bootstrap) batteries. These batteries provide energy for the X-day clocks and pyro functions.

Consideration is being given to developing a 60-day wet-life silver-zinc battery that would obviate the need for bootstrapping prior to entry. Although both power sources are considered to be suitable for a Jovian entry, the latter would be simpler and therefore less prone to unreliable operation. Its development for a 1980 mission is believed to be feasible.

Thermal Control - During subsonic descent, the warm heat shield provides a source of thermal energy which is inhibited by an insulation barrier built into the honeycomb structure. The ambient environment which ranges from a low of 144 K (-200 degrees F) at the start of descent to 422 K (+300 degrees f) at the 10 atmosphere level. Entry is considered to be at 1000 km. Analysis of the probe's thermal response during descent required formulation of a multi-node thermal model of the probe structure and equipment and representation of

all of the modes of heat transfer. An early 66 node model is being expanded to include the new science requirements and changing transmitter power levels. The choice of nodes was predicated on maintaining the number of nodes to within a manageable size while including adequate numbers of nodes at critical areas. Thus, over half of the nodes went into representing the forebody heat shield because of the steep temperature gradients developed during hypersonic entry within it.

Figure 28 shows the major elements of the thermal control subsystem schematically. The multilayer insulation (MLI) blanket and radioisotope heater

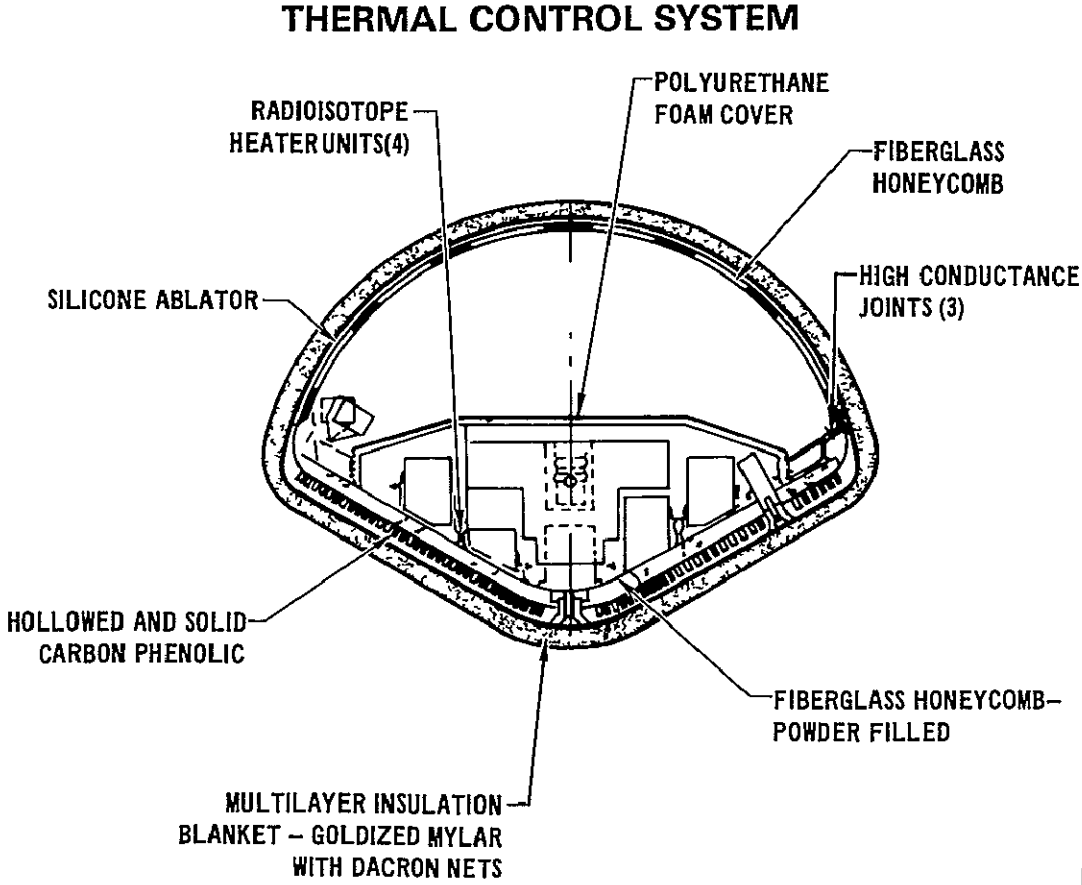

Figure 28

units (RHU's) provide passive thermal control during the long interplanetary journey and after separation. While still attached, the spacecraft augments the probe thermal control subsystem by controlling heat flow at the probe-adapter attachment points with an electrical heater and radiation surfaces on the adapter section. The entry heat protection system dissipates the high heating rates encountered during planetary entry as it descends in the atmosphere.

Little of the stored heat actually reaches the interior equipment section. A polyurethane foam cover forms the aft closure on the equipment bay and supports the microstrip antenna, however, controlled venting is permitted during Earth ascent and Jovian descent so pressure differentials remain small.

The heat shield temperature distribution, subsequent to aerodynamic heating, forms the initial boundary condition for the atmospheric descent portion of the thermal analysis. As the probe descends into the dense, relatively cold atmosphere, the heat shield surface cools very rapidly and approaches the temperature of the ambient environment. The presence of a hydrogen-helium gas mixture and a steadily increasing atmospheric density result in high surface cooling rates that are 20 to 40 times greater than for Earth atmospheric descents. Thus, the major portion of the heat content of the heat shield flows back to the surface with only a small fraction being leaked to the interior by conduction, radiation, and internally by convection. Operation of the electronic equipment yields about 175 watts of electrical waste heat with the transmitter providing most of this heat. Ambient planetary gas vents into the probe cavity during descent and provides a form of convective gas flow internally which prevents hot spots. These heat transfer mechanisms are accounted for in the analysis. Figures 29 and 30 present some representative heat shield and internal equipment temperatures for a Jupiter entry into a Nominal model atmosphere from a -7.5 degree entry condition. As stated, the analytical model is being expanded to account for instruments added fore and aft of the equipment cover and for increasing power levels.

The thermal control system is designed to satisfy the thermal requirements of all mission phases. The subphases of the mission profile that are important in design are: (1) interplanetary flight phase of the probe while attached to the spacecraft, (2) the autonomous period as the probe approaches the planet after separation from the spacecraft, and (3) the entry and descent phase into the planet's atmosphere. The probe is subjected to external environments that range in temperature from nearly absolute zero during the interplanetary flight to incandescent temperatures during the short hypersonic to subsonic entry phase. The thermal control subsystem must provide protection from these environments and maintain the internally mounted equipment within specified temperature limits.

FOREBODY HEATSHIELD TEMPERATURES

OPP-11

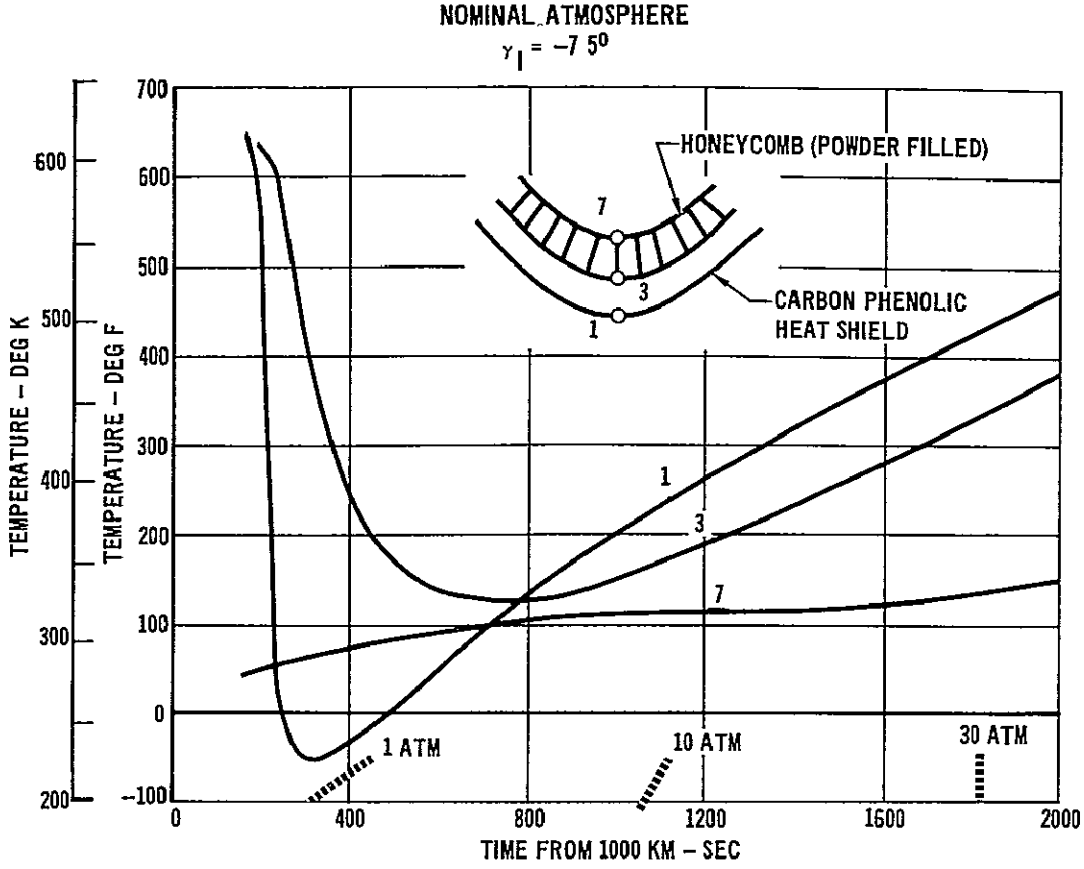

Figure 29

INTERNAL PROBE TEMPERATURES

OPP-10

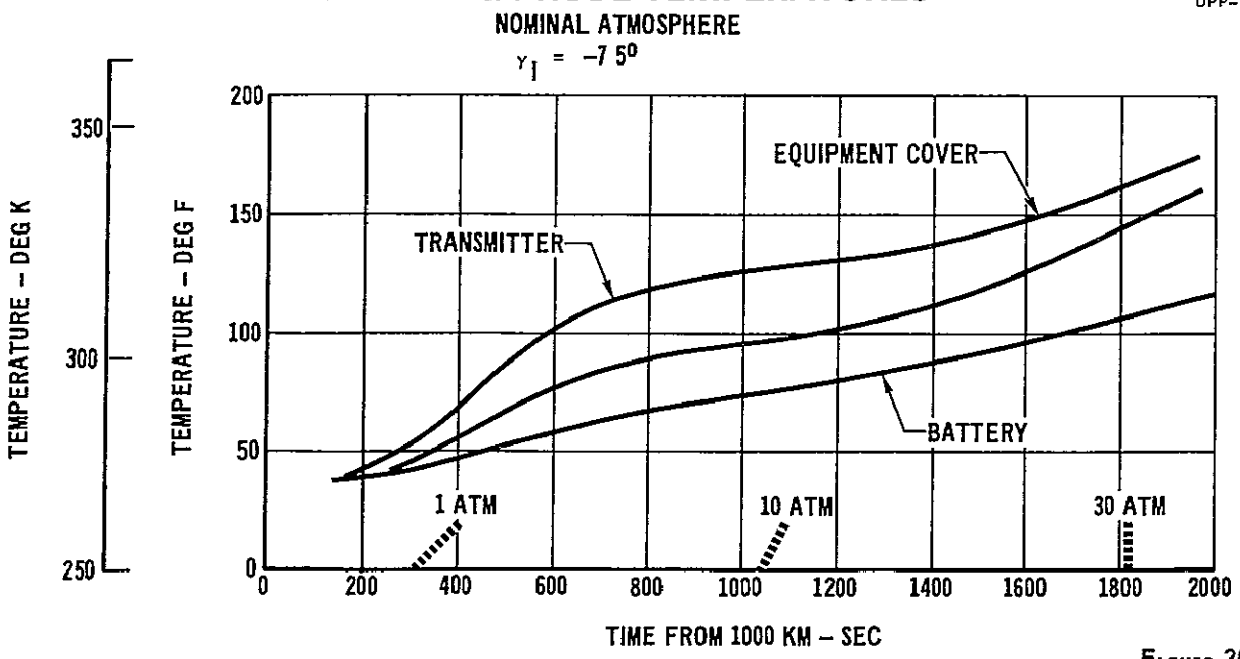

Figure 30

The thermal control subsystem is a simple, passive concept that maintains uniform temperatures inside during extremely-cold and extremely-hot phases of the mission. Validation of heat transport rates is underway: (1) the fiber-filled honeycomb rates are to be determined in laboratory tests, (2) a full-scale engineering model is under construction with built-in heat simulators, and (3) heat protection ablators are being tested for physical properties as well as for recession and erosion tendencies. RHU's have been used extensively on prior programs as have polyurethane foams. Their capabilities are well understood. A program of evaluating multilayer insulation heat retention capability has been formulated, but, again, use of the material in similar applications permits confident designing with only validation testing required in the Probe Development Phase.

CONCLUSIONS

The feasibility of an entry probe into Jupiter's atmosphere combined with an orbiter based on the Pioneer spacecraft is the subject of considerable interest. Definition of a different mission imposes new uncertainties as noted in Figure 31. Based on previously gathered analytical and test data, the 1980 opportunity has been studied preliminarily to ascertain the adaptability of a probe designed for Saturn and Uranus entry to one for Jupiter entry. It is concluded that the latter mission's requirements are compatible with the design of the former missions (see Figure 32). Changes in the heat shield thickness and the communication power level and, perhaps, frequency are required. The addition of instruments led to a reformatting of data as well as rearrangement of boxes, connectors and cabling. The net effect of these changes is an increase in power from earlier Jupiter entry studies that can be accommodated; a shift aft in center of gravity occurs which remains within acceptable dynamic stability boundaries; and an increase in heat load which may lead to the use of heavier gages in black-box thicknesses to enhance heat sink capability.

The two primary hazards, viz., trapped particle radiation and entry heat protection require continuing study to obtain optimal solutions. The equipment section is partially shielded by the plastic and metallic structures. Any added metal for heat sinking automatically enhances particle shielding. Care in timing of the entry can reduce the environment encountered by a factor of 4. Entry heat protection can be provided by using either current state-of-the-art laminated carbon phenolic or by near-term silica-silica heat shield materials.

A probe development schedule of three years or less is well balanced in terms of solving the important design problems early, validating all aspects of the spacecraft-probe combination prior to completion of flight hardware, and progressive fabrication of successively more sophisticated models by a single probe team. A program free from single-point bottlenecks and multiple back-ups is thereby achieved.

Thus, we conclude that the only major need for a successful launch, transit and entry is the authority to proceed with the program.

NEW MISSION UNCERTAINTIES

OPP-35

• TRAJECTORIES	ENTRY CONDITIONS PHASING TIME COMMUNICATIONS GEOMETRY ORBITER COMPATIBILITY
• ENVIRONMENT	TRAPPED PARTICLE MISSION DURATION
• ATMOSPHERIC DESCENT	DYNAMIC STABILITY ABLATION RATES THERMAL HISTORY
• COMMUNICATION LINK	LOSSES & TOLERANCES FREQUENCIES DATA RATES PREENTRY STORES
• SCIENCE	OBJECTIVES INSTRUMENTATION & COMMUNICATIONS
• ENERGY SOURCE	POWER PROFILE MISSION DURATION

Figure 31

CONCLUSIONS

OPP-20

• DEVELOPMENT OF A JUPITER PROBE	34–36 MONTHS (1979 OR 1980)
• ORBIT INSERTION	6 MINUTES AFTER END OF PROBE MISSION
• TRAPPED PARTICLE RADIATION	SURVIVAL PREDICTED, HARDENING/SHIELDING REQUIRED
• ENTRY ACCURACY	± 0 5^0 OF AIMPOINT
• ENTRY HEATING PROTECTION	LAMINATED CARBON-PHENOLIC OR SILICA-SILICA
• SCIENCE PAYLOAD	PRE-ENTRY STORED POST ENTRY REAL-TIME AND STORE DUMPED
• STABILITY	SATISFACTORY AT α = 30^0, IMPROVED AT α = 0^0
• COMMUNICATIONS	GOOD WITH A 60 W, 44 BPS CONVOLUTIONALLY CODED RELAY LINK
• ELECTRICAL POWER	125 W-HOURS REQUIRED
• THERMAL CONTROL	INSULATION AND RADIOISOTOPE HEATER UNITS
• PYROTECHNICS	NASA SBASI OR EQUIVALENT
• INTERFACES – SPACECRAFT	SIMPLE, DEFINED EXCEPT FOR RECEIVER ANTENNA

Figure 32

REFERENCES

(a) OPP-25, Preliminary ESRO PJO_p'80 Telecommunications Design, C. A. Hinrichs, 7 November 1974, McDonnell Douglas Astronautics Company.